JACS
JOURNAL OF THE AMERICAN CHEMICAL SOCIETY
Article
pubs.acs.org/JACS

Iron-Catalyzed Dehydrocoupling/Dehydrogenation of Amine–Boranes

James R. Vance, André Schäfer, Alasdair P. M. Robertson, Kajin Lee, Joshua Turner, George R. Whittell, and Ian Manners*

School of Chemistry, University of Bristol, Cantock's Close, Bristol BS8 1TS, U.K.

Supporting Information

ABSTRACT: The readily available iron carbonyl complexes, $[CpFe(CO)_2]_2$ (**1**) and $CpFe(CO)_2I$ (**2**) ($Cp = \eta$-C_5H_5), were found to be efficient precatalysts for the dehydrocoupling/dehydrogenation of the amine–borane $Me_2NH{\cdot}BH_3$ (**3**) to afford the cyclodiborazane $[Me_2N{-}BH_2]_2$ (**4**), upon UV photoirradiation at ambient temperature. In situ analysis of the reaction mixtures by ^{11}B NMR spectroscopy indicated that different two-step mechanisms operate in each case. Thus, precatalyst **1** dehydrocoupled **3** via the aminoborane $Me_2N{=}BH_2$ (**5**) which then cyclodimerized to give **4** via an off-metal process. In contrast, the reaction with precatalyst **2** proceeded via $Me_2NH{-}BH_2{-}NMe_2{-}BH_3$ (**6**) as the key intermediate, affording **4** as the final product after a second metal-mediated step. The related complex $Cp_2Fe_2(CO)_3(MeCN)$ (**7**), formed by photoirradiation of **1** in MeCN, was found to be a substantially more active dehydrocoupling catalyst and not to require photoactivation, but otherwise operated via a two-step mechanism analogous to that for **1**. Significantly, detailed mechanistic studies indicated that the active catalyst generated from precatalyst **7** was heterogeneous in nature and consisted of small iron nanoparticles (≤10 nm). Although more difficult to study, a similar process is highly likely to operate for precatalyst **1** under photoirradiation conditions. In contrast to the cases of **7** and **1**, analogous experimental studies for the case of photoactivated Fe precatalyst **2** suggested that the active catalyst formed in this case was homogeneous. Experimental and computational DFT studies were used to explore the catalytic cycle which appears to involve amine–borane ligated $[CpFe(CO)]^+$ as a key intermediate.

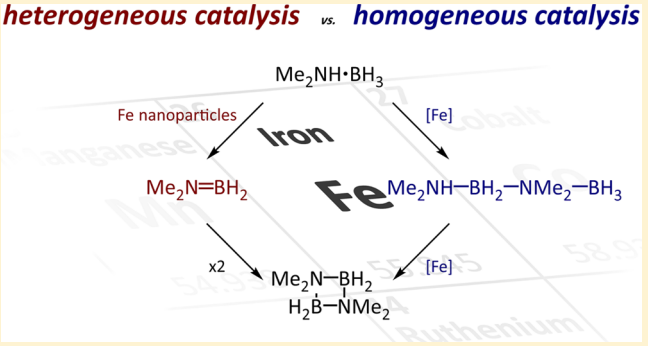

INTRODUCTION

Transition-metal complexes catalyze a broad spectrum of important organic transformations, and detailed mechanistic studies have revealed the importance of both homogeneous and heterogeneous processes.[1−6] A notable feature of recent work in this field has been a drive to replace the more prevalent "precious" metal catalysts with cheaper, more earth-abundant metals such as Ti, Ni, Co, and Fe.[7−10] By comparison with organic reactions, the corresponding use of metal-catalyzed transformations for main group substrates is in its relative infancy despite many significant advances.[11−14]

Amine–boranes, $R_xNH_{3-x}{\cdot}BH_3$ (R = H, alkyl, aryl), are readily (and in some cases commercially) available examples of main group coordination compounds and are widely used as either reducing[15−18] or hydroboration reagents.[19,20] In recent years, however, interest in amine–boranes and their derivatives[21−69] has attracted rapidly expanding attention due to potential uses in chemical hydrogen storage,[21−25] transfer hydrogenations and reductions of organic substrates,[26−32] and as precursors to polymeric and solid-state materials.[33−37,41] For example, $NH_3{\cdot}BH_3$ (**9**), which is an air- and moisture-stable solid of ∼20% gravimetric hydrogen content, has been the subject of intense interest worldwide as a portable source of hydrogen.[21−24] In addition, primary amine–boranes, $RNH_2{\cdot}BH_3$ (R = Me, nBu) (Scheme 1(i)) and **9**, have been shown to function as precursors to soluble polyaminoboranes[33−35,45] and also to "white graphene", which consists of a monolayer film of

Scheme 1. Metal-Catalyzed Dehydrocoupling/Dehydrogenation Pathways for (i) Primary and (ii) Secondary Amine–Boranes

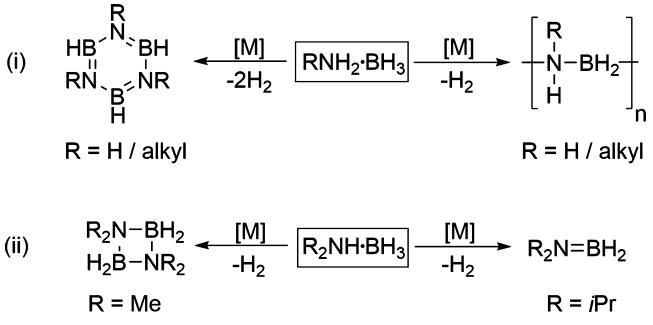

Received: October 2, 2013
Published: February 14, 2014

   dx.doi.org/10.1021/ja410129j | J. Am. Chem. Soc. 2014, 136, 3048−3064

Scheme 2. Dehydrogenation of $Me_2NH{\cdot}BH_3$ (3) via (i) $Me_2N{=}BH_2$ (5) (Off-Metal) or (ii) $Me_2NH{-}BH_2{-}NMe_2{-}BH_3$ (6) (On-Metal) with Regard to the Final Step to form $[Me_2N{-}BH_2]_2$ (4)

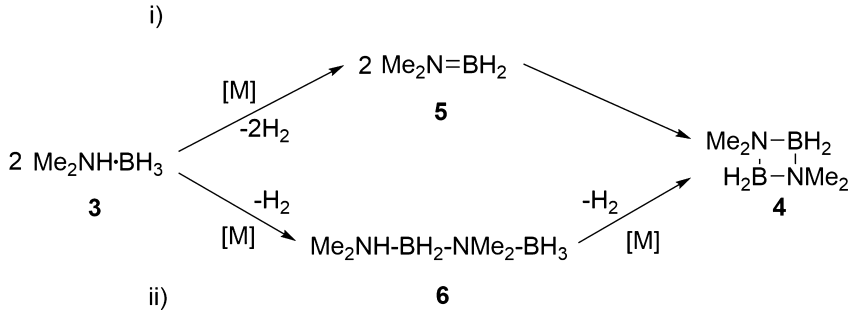

hexagonal boron nitride.[36] Of crucial relevance to the aforementioned applications are efficient protocols for the dehydrogenation of amine–boranes,[38] and substantial progress has been made in the field of metal-catalyzed reactions (Scheme 1).[39−66]

Amine–borane dehydrogenation catalysts that are based on metals from much of the periodic table have now been reported, but notably, if not unsurprisingly, almost all are 4d or 5d elements and many of these are "precious metals".[41,42,46,50,52,62,67,68] The development of catalysts based upon less expensive metals is therefore of major interest, and several examples based on earth abundant elements have now been published.[39,40,43,44,48,51,53−57,69] Systems based on Fe are of particular interest, and the first such example, $FeH(PMe_2CH_2)(PMe_3)_3$, was described briefly by Baker in 2007. In this case, high conversion of **9** to various dehydrocoupled oligomers was observed using 10 mol % catalyst after 4 days in THF at 20 °C.[47] In 2011, we reported our preliminary results on the use of photoactivated $[CpFe(CO)_2]_2$ (**1**) (5 mol %, 10 mol % Fe) in the catalytic dehydrogenation of **9** at 20 °C over 4 h in THF.[53] We also found that **1** is a rare example of a dehydrocoupling catalyst with significant activity toward a range of amine–boranes. For example, treatment of the primary amine–borane $MeNH_2{\cdot}BH_3$ (**10**) and the secondary amine–borane **3** with catalytic quantities of **1** also led to dehydrogenation to form various oligomeric and polymeric products. Recently, Baker et al. have also reported details on a series of mixed N–P donor ligated Fe(II) precatalysts with significant activity for the dehydrogenation of **9** with high conversion using 5 mol % catalyst in THF at 20–60 °C.[48,70] Furthermore, Morris et al. have recently demonstrated the use of Fe complexes such as *trans*-$[Fe(NCMe)CO(PPh_2C_6H_4CH{=}NCHPh)_2][BF_4]_2$ as precatalysts for the dehydrocoupling of both **3** and **9** in THF using 2.5 mol % catalyst in 1 h at 22 °C.[49] This report focused on the identification of the active catalyst which was proposed to be heterogeneous based on electron microscopy imaging of reaction mixtures and the similar behavior detected to that for previously studied transfer hydrogenation systems. Nevertheless, the acquisition of further evidence to support dehydrogenation by Fe nanoparticles was hindered by the rapid initial rates which obstructed any in operando studies.[49]

As part of the drive to improve fundamental understanding and catalyst efficiency, various experimental and computational studies have attempted to elucidate the mechanism(s) of metal-catalyzed amine-borane dehydrogenation.[39,40,44,50,52,55,71−73] Most of these studies have focused on the secondary amine–boranes $Me_2NH{\cdot}BH_3$ (**3**) (Scheme 1 (ii)) and $^iPr_2NH{\cdot}BH_3$ as substrates due to the formation of a single final product in very high yield, allowing them to be treated as simple model substrates for other amine–boranes. Even for amine–borane **3**, however, at least two metal-mediated mechanisms of H_2 release have been identified. Dehydrogenation is believed to occur either via the monomeric aminoborane, $Me_2N{=}BH_2$ (**5**), or the linear diborazane, $Me_2NH{-}BH_2{-}NMe_2{-}BH_3$ (**6**), invoking initial (i) intra- and (ii) intermolecular H_2 release steps, respectively (Scheme 2). The mechanism of dehydropolymerization of the primary amine–borane $MeNH_2{\cdot}BH_3$ (**10**) has also been studied, and although this will not be discussed in detail here, it is believed to involve a metal-centered dehydrogenation to form $MeNH{=}BH_2$ (**11**) followed by a second "on-metal" coordination polymerization step.[35,74]

In this paper, we report full details of our studies on photoactivated Fe complex **1** and other readily accessible and related iron carbonyl species as amine–borane dehydrogenation catalysts, focusing on a mechanistic investigation of the catalytic dehydrocoupling of **3**. In addition, we also report the development of an Fe precatalyst (**7**) that does not require photoactivation and that exhibits even higher activity. Our studies provide clear evidence that subtle structural differences in the precatalyst can lead to either heterogeneous or to homogeneous dehydrocoupling mechanisms that involve active catalysts that operate under mild conditions.

RESULTS

1. Dehydrocoupling of $Me_2NH{\cdot}BH_3$ (3) with Fe Complexes. With a view to extending the range of known Fe precatalysts for amine–borane dehydrogenation, we investigated the activity of various photoactive carbonyl complexes, beginning our studies with $[CpFe(CO)_2]_2$ (**1**) for which we have briefly reported preliminary results.[53] Addition of **1** (5 mol %, 10 mol % Fe) to the model amine–borane **3** in THF under photoirradiation led to rapid catalytic turnover, with quantitative conversion to the cyclic diborazane $[Me_2N{-}BH_2]_2$ (**4**) over 4 h at 20 °C. It is noteworthy that the relative activity of **1** was high when compared to the other potential precatalysts investigated. Furthermore, only $CpFe(CO)_2X$ [X = I (**2**) or Cl (**12**)] also produced a respectable rate of dehydrogenation under photoirradiation, with both precatalysts reaching ca. 60% conversion of **3** in toluene after 4 h, conditions under which the analogous use of **1** led to reaction completion (20 °C, 5 mol %) (Table 1).[75]

The respectable rates of dehydrogenation of **3** in the cases of photoirradiated precatalysts **1** and **2** encouraged us to initially focus on detailed studies solely of these two systems. Although a respectable rate of dehydrogenation was also observed using

dx.doi.org/10.1021/ja410129j | J. Am. Chem. Soc. 2014, 136, 3048−3064

Table 1. Dehydrocoupling Activity of Various Fe Complexes toward $Me_2NH{\cdot}BH_3$ (3) at 20 °C[a]

precatalyst (5 mol %)	time (h)	solvent	yield of $[Me_2N{-}BH_2]_2$ (4) (%)[b,c]
$[CpFe(CO)_2]_2$ (1)	4	THF	0
$[CpFe(CO)_2]_2$ (1)	4 ($h\nu$)	THF (Tol[d])	100 (80[e])
$[CpFe(CO)_2]_2$ (1)	4 ($h\nu$)	THF	55[f]
$[Cp^*Fe(CO)_2]_2$ (1*)	4 ($h\nu$)	THF	0
$[Cp^*Fe(CO)_2]_2$ (1*)	24 ($h\nu$)	THF	30
$Fe_2(CO)_9$ (8)	4 ($h\nu$)	THF	0
$Fe_3(CO)_{12}$	4 ($h\nu$)	THF	0
$CpFe(CO)_2I$ (2)	24	Tol	0
$CpFe(CO)_2I$ (2)	4 ($h\nu$)	THF (Tol)	30 (55)
$CpFe(CO)_2Cl$ (12)	24	Tol	0
$CpFe(CO)_2Cl$ (12)	4 ($h\nu$)	THF (Tol)	0 (65)
$FeCl_2$	4	THF	0
$FeCl_3$	4	THF	0

[a]Concentration of 3: 0.11 M. [b]Yield based on analysis by ^{11}B NMR spectroscopy. [c]Small amounts of $HB(NMe_2)_2$ (<5%) were also detected by ^{11}B NMR spectroscopy. [d]Reaction performed in toluene. [e]Although analysis by ^{11}B NMR spectroscopy showed only 80% conversion to 4, there was no starting material remaining in the reaction mixture as it was also converted to $HB(NMe_2)_2$.[76] [f]The reaction was repeated using 2.5 mol % of precatalyst 1 (therefore 5 mol % of Fe) to allow a direct comparison with the mononuclear Fe precatalysts.[77]

precatalyst **12**, this species is structurally very similar to precatalyst **2**, which, unlike **12**, is commercially available.

2. Observation of Intermediates in the Catalytic Dehydrocoupling of $Me_2NH{\cdot}BH_3$ (3) with Photoactivated $[CpFe(CO)_2]_2$ (1). Treatment of amine–borane **3** with Fe complex **1** (5 mol %) in THF at 20 °C in the absence of photoirradiation yielded no detectable dehydrocoupling over 4 h, and minimal dehydrocoupling over 24 h, based on analysis by ^{11}B NMR spectroscopy. However, rapid virtually quantitative dehydrocoupling to cyclic diborazane **4** (δ_B 4.1 ppm, t, J_{BH} = 113 Hz)[42] was observed by ^{11}B NMR spectroscopy over 4 h under photoirradiation conditions, where the escape of the gaseous byproducts (presumably H_2 and CO, Scheme 3) was

Scheme 3. Dehydrogenation of $Me_2NH{\cdot}BH_3$ (3) with Photoactivated $[CpFe(CO)_2]_2$ (1) (5 mol %) To Form $[Me_2N{-}BH_2]_2$ (4)

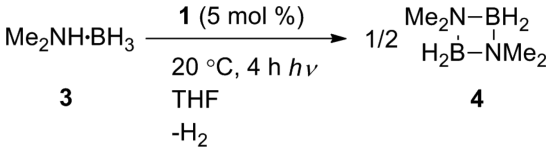

allowed. A reduced rate (80% conversion to **4** over 6 h) was observed when the reaction was performed in a closed system, with the rate likely being limited by competitive coordination of released H_2 and/or CO to the photogenerated catalyst. All subsequent reactions were therefore performed in open systems, under nitrogen on a Schlenk line. Interestingly, photoirradiation of precatalyst **1** for 1 h in THF before subsequent addition of amine–borane **3** led to no conversion after 3 h when analyzed by ^{11}B NMR spectroscopy, indicating that the presence of the amine–borane was essential in the formation of the active catalyst.

Monitoring the reaction of **3** with precatalyst **1** (5 mol %, THF) by ^{11}B NMR spectroscopy also provided mechanistic insight into the dehydrocoupling process. During the course of the reaction, in addition to the growing peak at 4.1 ppm associated with the final dimeric product **4**, a new resonance was detected at δ 36.5. This was assigned to the monomeric aminoborane **5**, based on the chemical shift and the triplet multiplicity ($^1J_{BH}$ = 127 Hz) in the ^{11}B NMR spectrum (Figure 1).[72]

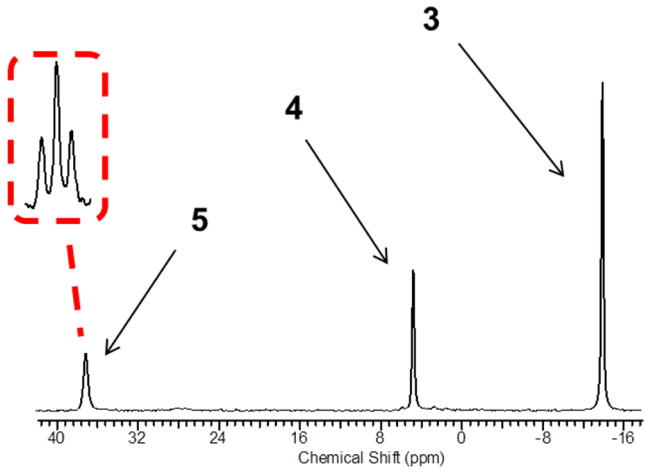

Figure 1. $^{11}B\{^1H\}$ NMR spectrum of the reaction mixture derived from photoirradiated $[CpFe(CO)_2]_2$ (1) (5 mol %) and $Me_2NH{\cdot}BH_3$ (3) (30 min, THF, 20 °C). Inset illustrates triplet multiplicity of the peak at δ 36.5 in the corresponding ^{11}B NMR spectrum.

Significantly, the linear diborazane **6** [δ_B −13.7 (q, $^1J_{BH}$ = 94 Hz, BH_3), 1.4 (t, $^1J_{BH}$ = 108 Hz, BH_2)],[78] noted earlier as a key intermediate in many other proposed catalytic cycles (Scheme 2), was not detected in significant amounts by ^{11}B NMR spectroscopy during the reaction of **3** with photoirradiated **1**. In addition, separate experiments showed that **1** was virtually inactive (<5% conversion to **4**) toward dehydrocoupling of independently synthesized **6**, even upon photoirradiation for 21 h. The absence of linear diborazane **6** as an intermediate was further demonstrated upon treatment of an equimolar mixture of $Me_2NH{\cdot}BD_3$ (**3**-d_3) and **6** with **1** (5 mol %) under photoirradiation (4 h, THF, 20 °C). Analysis of the resulting mixture by ^{11}B NMR spectroscopy indicated that while **3**-d_3 was converted to $[Me_2N\text{-}BD_2]_2$ (**4**-d_4), **6** was left unreacted (Scheme 4, Figure 2), further underlining the lack of reactivity of this substrate toward photoactivated **1**.

3. Observation of Intermediates in the Catalytic Dehydrocoupling of $Me_2NH{\cdot}BH_3$ (3) with Photoactivated $CpFe(CO)_2I$ (2). Following the investigation of precatalyst **1**, the reactivity of Fe precatalyst **2** toward **3** was studied in detail. Treatment of **3** with precatalyst **2** (5 mol %, toluene, 20 °C) under photoirradiation led to virtually quantitative dehydrogenation over 9 h to form the cyclic diborazane **4**, as evidenced by ^{11}B NMR spectroscopy. Remarkably, however, monitoring the reaction indicated very different mechanistic behavior compared to that exhibited by the reaction of precatalyst **1** with the same substrate. In the case of **2**, and in contrast to that with **1**, the linear diborazane **6** was detected in significant quantity by ^{11}B NMR spectroscopy [δ_B

dx.doi.org/10.1021/ja410129j | J. Am. Chem. Soc. 2014, 136, 3048–3064

Scheme 4. Attempted Dehydrogenation of a Mixture of $Me_2N{-}HBH_2{-}NMe_2BH_3$ (6) and $Me_2NH{\cdot}BD_3$ (3-d_3) with Photoirradiated $[CpFe(CO)_2]_2$ (1) (5 mol %)

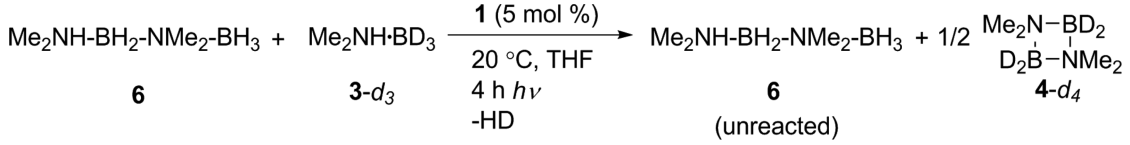

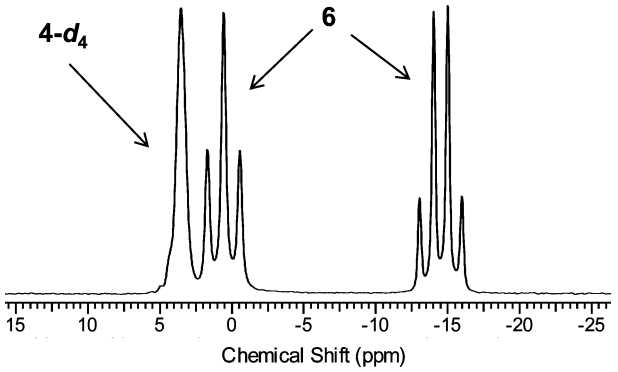

Figure 2. ^{11}B NMR spectrum of the reaction of photoactivated $[CpFe(CO)_2]_2$ (**1**) (5 mol %) with $Me_2NH{-}BH_2{-}NMe_2{-}BH_3$ (**6**) and $Me_2NH{\cdot}BD_3$ (**3**-d_3) (4 h, THF, 20 °C) affording $[Me_2N{-}BD_2]_2$ (**4**-d_4) as the final product where **6** is left unreacted.

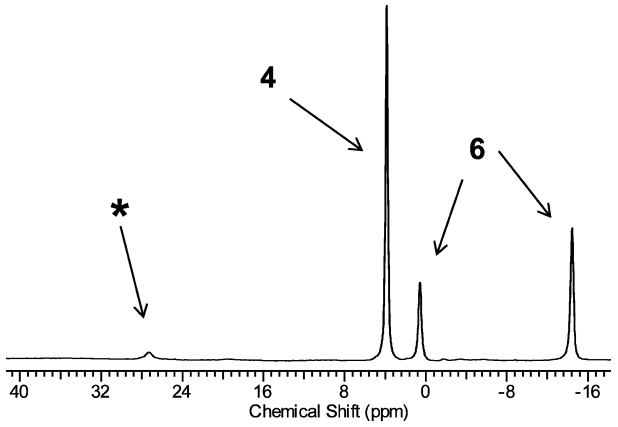

Figure 3. $^{11}B\{^1H\}$ NMR spectrum of the reaction of photoactivated $CpFe(CO)_2I$ (**2**) (5 mol %) and $Me_2NH{\cdot}BH_3$ (**3**) (5 h, toluene, 20 °C) affording $[Me_2N{-}BH_2]_2$ (**4**) as the final product, via $Me_2NH{-}BH_2{-}NMe_2{-}BH_3$ (**6**). The signal labeled with * is assigned to $HB(NMe_2)_2$.

−13.7 (q, $^1J_{BH}$ = 94 Hz, BH_3), 1.4 (t, $^1J_{BH}$ = 108 Hz, BH_2)][78] (Scheme 5 and Figure 3), and the monomeric aminoborane **5** (δ_B 36.5 ppm) was virtually absent. These results suggested that an alternative mechanism was operational when photoactivated **2** was employed as the precatalyst.

To further probe the mechanism of the dehydrogenation in this case, the catalytic reaction of linear diborazane **6** with **2** was also explored. Treatment of a toluene solution of **6** with **2** (5 mol %) under photoirradiation led to 47% conversion to **4** over 4 h at 20 °C based on analysis by ^{11}B NMR spectroscopy. The rate of dehydrocyclization of isolated linear diborazane **6** with photoactivated **2** is consistent with the former species functioning as a key intermediate in the catalytic dehydrogenation of **3** to afford **4** which takes 9 h to reach completion. This observation was in marked contrast to the behavior of the related Fe complex **1**, which was shown to dehydrocouple **3** via the monomeric aminoborane **5** as the key intermediate and to be virtually inactive toward **6**. The reactions with **3** and **6** were also repeated with $CpFe(CO)_2Cl$ (**12**), which demonstrated very similar reactivity in toluene to that observed in the case of **2**.

4. Nature of the Active Catalysts in the Catalytic Dehydrogenation of 3 Using $[CpFe(CO)_2]_2$ (1) and $CpFe(CO)_2I$ (2) as Precatalysts. The mechanisms of dehydrogenation of amine−borane **3** by complexes **1** and **2** appear to be fundamentally different as distinct intermediates are detected in each case. However, the necessity of photoirradiating both species to induce catalytic activity somewhat hampers a detailed experimental investigation of the contrasting mechanisms. Nevertheless, it can be assumed that in each case photoirradiation leads to the cleavage of one or more bonds at the respective Fe center leading to coordinative unsaturation, thus facilitating the formation of a catalyst that permits amine−borane coordination and entry into the catalytic manifold.

(a). $[CpFe(CO)_2]_2$ (1) as Precatalyst. Previous work has shown that, in the case of precatalyst **1**,[79] photoirradiation leads to two distinct bond activation processes. These involve carbonyl dissociation to form the coordinatively unsaturated dinuclear species $[Cp_2Fe_2(CO)_3]$ and homolytic cleavage of the central Fe−Fe bond to form two $[CpFe(CO)_2]$ radicals.[80−82] The formation of both products has been reported to occur under a variety of conditions. Moreover, the former species has been shown to form adducts with simple 2-electron donors, e.g., PPh_3, and the latter found to be capable of atom abstraction reactions. Indeed, both of the photogenerated iron species could react directly with amine−boranes, which have been shown to bind to coordinately unsaturated metal centers via the hydride substituents at boron[59,67,83−86] and also to undergo hydride abstraction to form boron-centered cations[87] and to participate in radical reactions.[87−89] Although it was not

Scheme 5. Dehydrogenation of $Me_2NH{\cdot}BH_3$ (3) with Photoactivated $CpFe(CO)_2I$ (2) (5 mol %) To Form $[Me_2N{-}BH_2]_2$ (4)

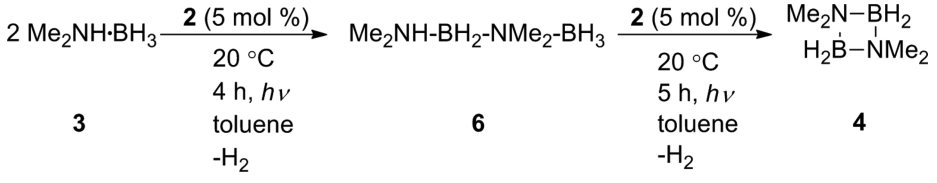

dx.doi.org/10.1021/ja410129j | J. Am. Chem. Soc. 2014, 136, 3048−3064

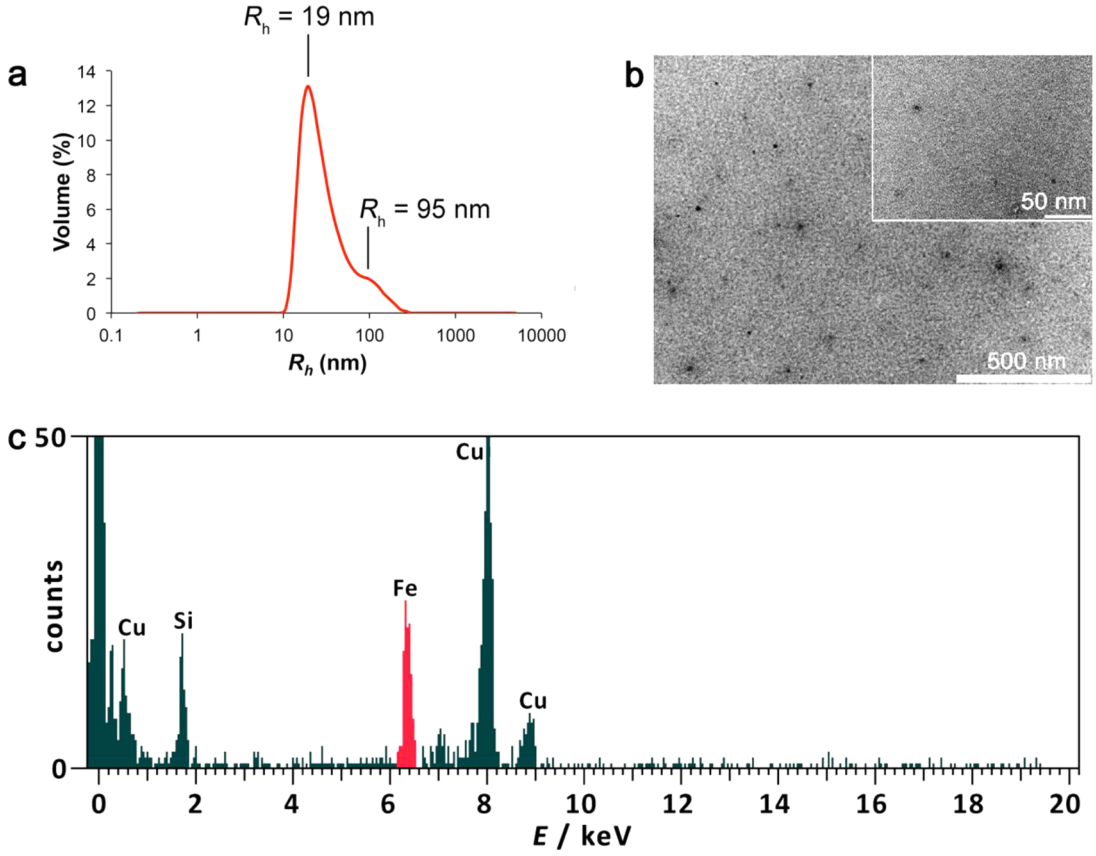

Figure 4. (a) DLS particle size distribution by volume. (b) TEM micrograph showing evidence for the colloidal nature of the reaction of $Me_2NH{\cdot}BH_3$ (**3**) and $[CpFe(CO)_2]_2$ (**1**) (5 mol %) after photoirradiation (insert: higher magnification image). (c) Energy dispersive X-ray spectroscopic (EDX) analysis of the particles (probe size diameter: 35 nm). The Cu in the EDX spectrum arises from the TEM grid on which the sample was analyzed, while we propose that the Si arises from silicone grease present in the reaction mixture.

possible to directly distinguish between the two possible reactive species in the reaction of **3** with photoactivated **1**, it is noteworthy that $[Cp_2Fe_2(CO)_3]$, the product of CO dissociation, is known to have a greater solution lifetime than that of $[CpFe(CO)_2]$.[79,90]

With respect to the mechanism for precatalyst **1**, it was conceivable that photoirradiation might only be required to initiate catalysis, with the reaction then continuing after irradiation has been halted. To probe this possibility, a solution of **3** in THF was irradiated in the presence of 5 mol % **1** over 1 h, before analysis by ^{11}B NMR spectroscopy. At this point, ~50% conversion of **3** was apparent. The mixture was then stirred at ambient temperature without further photoirradiation for 3 h, while monitoring by ^{11}B NMR spectroscopy, during which time the reaction reached completion. Therefore, it was clear that photoirradiation was not required throughout the reaction to achieve catalytic turnover.[91]

Various methods exist for differentiating between homo- and heterogeneous catalysis, with seminal contributions in the area from Finke and co-workers.[92−94] Two of the most important tests used to distinguish between these catalysts are (a) kinetic studies to investigate the presence of an induction period (vide supra) and (b) monitoring the effects of selective poisoning and filtration. With respect to kinetic measurements, the generation of the active catalyst under photolysis conditions precluded accurate monitoring of the initial stages of the reaction by ^{11}B NMR spectroscopy, although later stages of the reaction could be monitored. Photoirradiation also made selective poisoning experiments non-trivial to perform. For these experiments, most commonly a phosphine or related donor is employed as a potential poison for the active catalytic sites, with the stoichiometry required to completely halt the reaction being key to distinguishing between a heterogeneous or homogeneous process. Thus, for a homogeneous process, assuming a single active site per complex, a stoichiometric quantity of phosphine relative to catalyst would be needed to completely curtail catalysis. In contrast, in the case of a heterogeneous system, a substoichiometric quantity is sufficient due to the relatively small fraction of metal centers actually available for catalysis at the metal surface.

To explore selective poisoning, amine−borane **3** was treated with precatalyst **1** (5 mol %) at 20 °C in THF under photoirradiation for 1 h. Analysis by ^{11}B NMR spectroscopy indicated ~50% conversion to **4** after the allotted time. The reaction mixture was then divided in two, with one sample (i) treated with 0.1 equiv of PMe_3 (relative to **1**) and the other (ii) left unchanged. After a further 3 h with no photoirradiation, the two samples were again analyzed by ^{11}B NMR spectroscopy, with (i) showing no further conversion indicting complete suppression of catalysis and (ii) showing 100% conversion to **4**. These results are consistent with the presence of a heterogeneous, colloidal Fe nanoparticle catalyst rather than an active homogeneous species.

To further probe the nature of the active catalyst, dynamic light scattering (DLS) studies were performed. DLS is a technique used for determining the size of particles in a

dx.doi.org/10.1021/ja410129j | J. Am. Chem. Soc. 2014, 136, 3048−3064

colloidal solution. In the context of this research, DLS is particularly useful as it can be used to confirm the heterogeneity of a catalytic reaction by the detection of metal colloid particles. Furthermore, the technique can be applied to samples under an inert atmosphere and in a broad range of common solvents. A solution of precatalyst **1** (5 mol %) and amine−borane **3** in THF was photoirradiated for 1 h to ensure the formation of the catalytically active species and was then analyzed by DLS. The resulting volume distribution, derived from a distribution fit of the correlation function (see the Supporting Information, Figures S1 and S2), demonstrated the presence of colloidal species in solution. Specifically, a population of particles was detected centered at a hydrodynamic radius, R_h, of 19 nm with a minor contribution at larger size (R_h = ca. 95 nm) (Figure 4a). An aliquot was subsequently removed and dropped onto a carbon-coated copper grid for analysis by transmission electron microscopy (TEM). The images obtained (e.g., Figure 4b) indicated the presence of particles with an average diameter of 7 nm which were confirmed to contain Fe by energy-dispersive X-ray spectroscopic (EDX) analysis (Figure 4c).[95] This result is broadly consistent with that obtained by DLS when both errors associated with surface coatings and solvation, which may not be evident by TEM, and the assumptions required to obtain R_h from the diffusion coefficient are considered.[96]

In order to exclude the possibility that the Fe nanoparticles were formed on exposure of the Fe complex to the electron beam during the TEM experiment, rather than being already present in the reaction mixture, a solution of **1** in THF was prepared and an aliquot drop-cast on a carbon-coated copper grid. Imaging by TEM revealed the presence of some particles (Figure S4(a), Supporting Information), albeit with considerably lower surface density on the grid than observed for the reaction mixture. Analysis of the same solution of **1** by DLS, however, afforded no evidence for the presence of particles within the experimentally detectable size range (R_h = 0.3 nm −10 μm) (see Figure S3, Supporting Information). This suggested that the nanoparticles observed at low surface density in the TEM image from the control solution (Figure S4(a), Supporting Information) were a product of the technique itself and were not inherent to the sample.

Another useful analytical technique for investigating the presence of a heterogeneous catalyst is UV−vis spectroscopy. This method can be used to detect the surface plasmon resonances associated with metallic nanoparticles, which appear as broad absorptions through the visible spectrum down to short wavelengths (below 400 nm).[97,98] However, the UV−vis spectrum obtained upon analysis of a reaction mixture containing precatalyst **1** (5 mol %) and amine−borane **3** in THF following photoirradiation (1 h) showed little change from that of a control sample of **1** in THF. This contrasts with the results of poisoning studies and TEM analysis which strongly indicate that the catalyst is heterogeneous. It is, however, likely that only a very small amount of the initial precatalyst **1** may be photoactivated and/or reduced to nanoparticles, which may lead to a minimal change in the UV−vis spectrum.

(b). CpFe(CO)$_2$I (2) as Precatalyst. As for the case of precatalyst **1**, the photochemistry of **2** has been extensively studied, with two major processes identified. These involve CO dissociation to form the neutral 16-electron complex [CpFe(CO)I][99,100] and heterolytic Fe−I bond cleavage to form the cationic 16-electron $[CpFe(CO)_2]^+$.[101,102] We therefore performed a number of experiments to investigate the differences between the active catalytic species formed by **1** and **2** under the reaction conditions.

As discussed above (section 4 (a)), we found that photoirradiation of **3** with **1** was only necessary to initiate catalysis with further dehydrogenation observed after photolysis had been halted. We performed analogous experiments to investigate whether precatalyst **2** exhibited similar behavior. Reaction of **3** with **2** (5 mol %) in toluene with photoirradiation for 4 h led to 60% conversion to **4** upon analysis by ^{11}B NMR spectroscopy. The reaction mixture was then stirred for 18 h in the absence of photoirradiation before further analysis by ^{11}B NMR spectroscopy. In this case and in contrast to that for **1**, no further conversion was detected demonstrating that continuous photoirradiation was necessary to achieve catalysis when using **2**.

As previously noted, the presence of a different intermediate compared to that observed with precatalyst **1** suggested the operation of a fundamentally different mechanism, and this is supported by the loss of catalytic activity after the cessation of photoirradiation. The same tests that indicated the active catalyst formed from **1** was heterogeneous were then repeated to probe the nature of the active species formed during the reaction of **3** with precatalyst **2** under photoirradiation. Thus, following partial (ca. 60% conversion) conversion of **3** to **4** mediated by 5 mol % of **2** in toluene after photoirradiation for 4 h, addition of 0.4 equiv of PMe_3 relative to catalyst followed by further photoirradiation led to continued, but slower, dehydrocoupling to yield **4** (ca. 80% total conversion after a further 3 h). When the reaction was repeated with 1 equiv of PMe_3, complete suppression of catalytic activity was observed. These results are in line with those expected for a homogeneous catalyst and contrast with those for **1**, where complete suppression of activity was detected with substoichiometric quantities of PMe_3 (e.g., 0.1 equiv). Furthermore, both TEM and DLS analysis of reaction solutions derived from the reaction of **3** with precatalyst **2** (5 mol %) in toluene also failed to show evidence for the presence of a significant concentration of Fe nanoparticles. For example, DLS analysis of the resulting mixture after 1 h (Figure S1, Supporting Information) suggested that the reaction mixture did not contain particles within the experimentally observable size range (R_h = 0.3 nm to 10 μm). Once again, the results for precatalyst **2** contrast with those obtained for precatalyst **1** and are strongly indicative of a homogeneous process in this instance.

To provide further insight into the nature of the active homogeneous catalyst and the potential role of CO and I^- ligand loss, we also explored the behavior of several related Fe carbonyl complexes as precatalysts. We already noted that the chloro analogue of **2**, complex **12**, showed similar activity for the dehydrogenation of **3** under photoirradiation (Table 1). Similarly, treatment of **3** with 5 mol % of $[CpFe(CO)_2(THF)][X]$ ($[X]^- = [BF_4]^-$ **13a**, $[SbF_6]^-$ **13b**) and $CpFe(CO)_2(OTf)$ (OTf = OSO_2CF_3) (**14**) in the presence of UV light in either THF or toluene also gave a conversion to **4** by ^{11}B NMR spectroscopy similar to that detected with **2** as the precatalyst (Table S2, Supporting Information). In addition, as observed with **2** as precatalyst, no catalytic activity was detected in the absence of photoirradiation, and the reactions with **12**, **13a** and **13b**, and **14** (Scheme 6) were all found to proceed via the linear diborazane **6** as an intermediate. Moreover, catalysis ceased when UV irradiation was halted in the cases of **12** and **14** (5 mol % precatalyst, toluene, 20 °C). In contrast, in the cases of **13a** and **13b**, which possess the weakly coordinating

dx.doi.org/10.1021/ja410129j | J. Am. Chem. Soc. 2014, 136, 3048−3064

Scheme 6. $CpFe(CO)_2I$ (2) and Related Complexes

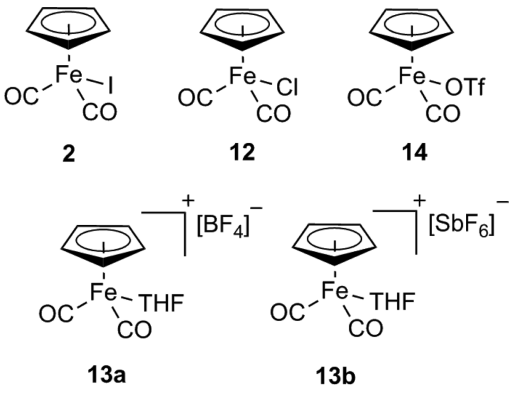

$[BF_4]^-$ and $[SbF_6]^-$ anions, respectively, slower but significant further conversion of **3** to **4** was detected (20% conversion after 2 h with UV light, with 60% further conversion after an additional 18 h when photoirradiation was halted in the case of **13a** and 40% further conversion in the case of **13b**).

The aforementioned observations with structurally related complexes suggest that loss of both CO and I^- from **2** may be necessary in order to generate the active homogeneous catalyst.[103] For example, the activity under UV irradiation of **13a** and **13b**, in which the organoiron cations already lack a halide ligand, is also strongly indicative of the need for CO loss. To explore this further, we investigated the effect of CO and I^- on the dehydrogenation of **3** with **2** as precatalyst. A THF solution of amine−borane **3** and **2** (5 mol %) was exposed to an atmosphere of CO, and the reaction mixture was photoirradiated for 4 h. Analysis by ^{11}B NMR spectroscopy showed only 5% conversion to **4** which was significantly less than observed under usual conditions with an N_2 atmosphere (60% conversion in 4 h). Subsequent replacement of CO by an atmosphere of N_2 together with photoirradiation for 16 h resulted in further high conversion of **3** to **4** (70%). To investigate the effect of I^- on the conversion rate, an equimolar quantity of $[n\text{-}Bu_4N]I$ and **3** was treated with **2** (5 mol %) in THF at 20 °C under photoirradiation for 4 h. This led to only 10% conversion to **4** upon analysis by ^{11}B NMR spectroscopy, much less than the ca. 60% conversion otherwise anticipated. The relative suppression of catalysis upon addition of CO or I^- provides further support for the need for photoinduced dissociation of both CO and I^- dissociation from **2** to generate the active catalyst. In addition, the observation that, once initiated, catalysis continues in the absence of further irradiation in the case of **13a** and **13b** but not for **2** may be a consequence of recoordination of the iodide anions at the metal center in the latter case. The reactions with added CO and I^- were also repeated with precatalyst **13b**. Similarly, reaction of **3** with **13b** (5 mol %) under an atmosphere of CO in toluene for 4 h with photoirradiation at 20 °C led to a suppression of catalytic activity based on analysis by ^{11}B NMR spectroscopy (5% conversion).[104] Upon replacing the atmosphere of CO with N_2 and photoirradiating for a further 18 h, 60% conversion of **3** to **4** was detected. Also, treatment of **3** and an equimolar amount of $[n\text{-}Bu_4N]I$ with **13b** (5 mol %) in THF at 20 °C under photoirradiation for 4 h led to minimal conversion to **4** (10%) upon analysis by ^{11}B NMR spectroscopy.

To provide further insight into the likely intermediates in the catalytic cycle for **2**, DFT calculations were performed on the chloro analogue **12** which behaves similarly.[105] Initially, we attempted to calculate possible intermediates based on the generation of the 16-electron species $[CpFe(CO)Cl]$ or $[CpFe(CO)_2]^+$, arising from either CO or halide loss from **12**, respectively. However, as these possible intermediates possess only a single vacant coordination site we found that complexes such as $[CpFe(CO)Cl(H_3BNMe_2H)_2]$ or $[CpFe(CO)_2(H_3BNMe_2H)_2]^+$, upon optimization, always led to the loss of one molecule of coordinated **3**. We, therefore, investigated species based on $[CpFe(CO)]^+$, the product from both CO and halide dissociation, as the key intermediate which is presumably formed in amine−borane ligand-stabilized form (**15**) (Scheme 7). This 14-electron complex offers two vacant coordination sites, and we examined a series of plausible intermediates that might arise from this species (Figure 5).[106]

The first coordination of 1 equiv of **3** to the $[CpFe(CO)_2]^+$ cation was found to be highly exergonic by −136.0 kJ·mol^{-1}, and the subsequent loss of one molecule of CO was calculated to be slightly exergonic by −7.1 kJ·mol^{-1}. The coordination of a second equivalent of **3** was found to be exergonic as well by

Scheme 7. Possible Processes in the Formation of the Active Catalyst from $CpFe(CO)_2I$ (2) in the Reaction with $Me_2NH{\cdot}BH_3$ (3) under Photoirradiation Conditions in an Open System

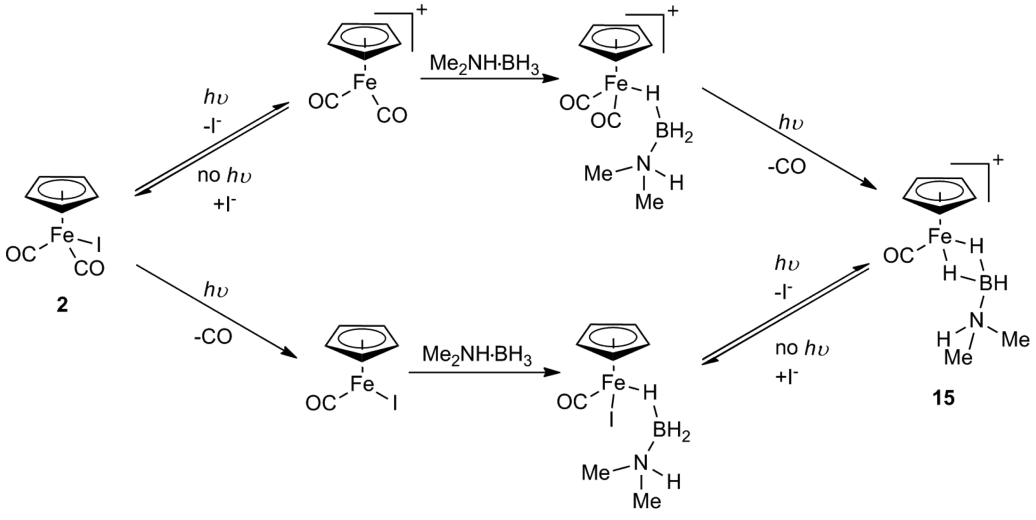

dx.doi.org/10.1021/ja410129j | J. Am. Chem. Soc. 2014, 136, 3048−3064

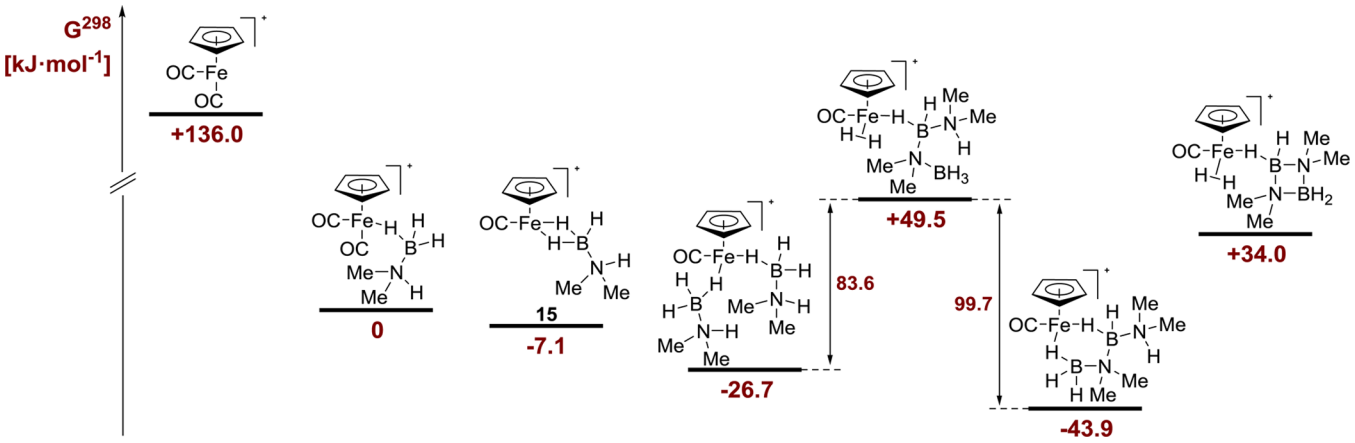

Figure 5. Calculated relative free enthalpies at 298 K (in kJ·mol^{-1}) for relevant intermediates of the reaction of $[CpFe(CO)_2]^+$ + **3** (all calculations performed for the formula $C_{11}H_{25}B_2FeN_2O_2$, respectively). Calculations were performed at the M06-2X/6-311G(d,p)(C, H, B, N, O);SDD(Fe) level of theory.

−19.6 kJ·mol^{-1}. In all cases, coordination to Fe through B−H groups was preferred over the N−H groups. The B−H/N−H bond cleavage and the B−N bond formation process is most likely the rate-determining step for the first part of the catalytic cycle in which the linear diborazane is generated. The overall reaction of $[CpFe(CO)_2]^+$ with two molecules of **3** to give the linear diborazane **6** coordinated to the metal is exergonic (by −43.9 kJ·mol^{-1}), while the subsequent step to form the coordinated cyclic diborazane **4** is endergonic (+77.9 kJ·mol^{-1}) and the formation of free **4** from **6** is exergonic (by −57.0 kJ·mol^{-1}). This is in agreement with the experimental observation that amine−borane **3** is first transformed to **6** and that only after most of the starting material has been consumed, conversion to the cyclic diborazane **4** as the final product is observed. Furthermore, these calculations, coupled with the aforementioned experimental results, are consistent with the loss of CO and halide to form the active catalytic species from **2**.

5. Studies of $Cp_2Fe_2(CO)_3(MeCN)$ (7): A Fe Precatalyst for Amine−Borane Dehydrogenation That Does Not Require Photoirradiation. Although compounds **1** and **2** are commercially available and relatively efficient precatalysts for the dehydrogenation of **3**,[107] the necessity for photoirradiation increased the complexity of the experimental setup and also limited the scope of the mechanistic studies. It was, therefore, highly desirable to identify related Fe complexes, for which photoirradiation was not a prerequisite for catalytic activity.

It has previously been demonstrated that the photoirradiation of Fe complex **1** in the presence of various two electron donors can lead to the formation of new species of the form $Cp_2Fe_2(CO)_3L$ [L = MeCN, PR_3, $P(OR)_3$].[108,109] If the new ligand is particularly weakly coordinating, under certain conditions it may dissociate to yield a coordinatively unsaturated species $Cp_2Fe_2(CO)_3$, a likely intermediate formed during the photoirradiation of precatalyst **1** in the presence of **3** [section 4 (a)]. The targeted complex $Cp_2Fe_2(CO)_3(MeCN)$ (**7**) was synthesized via a slight modification of the method reported by Labinger et al. through photolysis of **1** in MeCN solution (Scheme 8).[109] The compound was isolated as a green, highly air-sensitive solid and was subsequently stored at −40 °C under N_2. Analysis by ^{1}H, ^{13}C NMR spectroscopy and UV−vis spectroscopy confirmed the identity of the compound based on the previous reports with relatively rapid decomposition

Scheme 8. Synthesis of $Cp_2Fe_2(CO)_3(MeCN)$ (7)

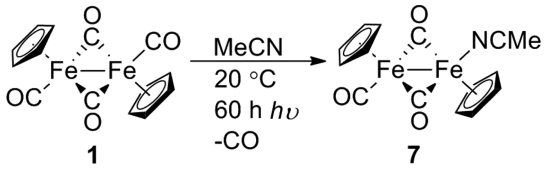

apparent in most solvents presumably instigated by MeCN dissociation. In contrast, precatalyst **7** was shown to be indefinitely stable in MeCN solution, presumably caused by inhibition of ligand dissociation due to the large excess of MeCN present.

To probe the reactivity of **7** as a precatalyst, amine−borane **3** was treated with 5 mol % of **7** at 20 °C in toluene under conditions analogous to those employed for complexes **1** and **2** except that photoirradiation was not used. The reaction mixture was subsequently monitored by ^{11}B NMR spectroscopy. Quantitative conversion to cyclic diborazane **4** was observed in only 20 min, confirming the very high activity of **7** as an amine−borane dehydrogenation precatalyst (Scheme 9). When

Scheme 9. Dehydrogenation of $Me_2NH{\cdot}BH_3$ (3) with $Cp_2Fe_2(CO)_3(MeCN)$ (7) (5 mol %) Forming $[Me_2N{-}BH_2]_2$ (4)

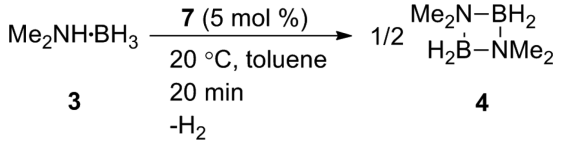

the activity of this complex was compared with other known dehydrocoupling catalysts for **3**, it was found that the rate of dehydrogenation was among the most rapid known for this transformation.[87,110] Interestingly, catalysis was found to be completely suppressed upon repeating the reaction in neat MeCN (16 h, 20 °C by ^{11}B NMR spectroscopy), presumably due to inhibition of the ligand loss necessary for the generation of the active catalytically species.[111]

Despite the rapid rate of dehydrogenation of amine−borane **3** with **7** as a precatalyst relative to that observed with complex **1**, the monomeric aminoborane **5** (δ_B 36.5 ppm) was again detected as an intermediate by ^{11}B NMR spectroscopy during

dx.doi.org/10.1021/ja410129j | J. Am. Chem. Soc. 2014, 136, 3048−3064

the course of the reaction (Figure 6). Furthermore, as with the case of **1**, linear diborazane **6** was not observed in significant

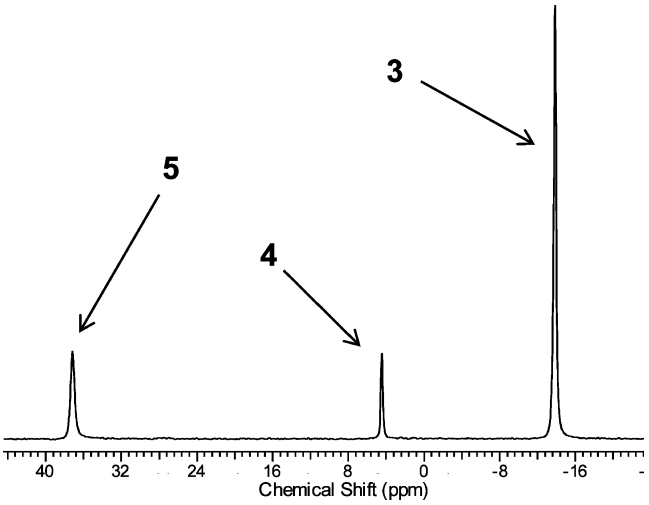

Figure 6. $^{11}B\{^1H\}$ NMR spectrum of the reaction mixture (toluene, 20 °C) derived from $Me_2NH{\cdot}BH_3$ (**3**) with $Cp_2Fe_2(CO)_3(MeCN)$ (**7**) (5 mol %) forming $[Me_2N{-}BH_2]_2$ (**4**) via $Me_2N{=}BH_2$ (**5**) after 10 min.

amounts. In line with these results, separate experiments also showed that **7** was virtually inactive toward the dehydrogenation of **6** with less than 5% conversion to cyclic diborazane **4** detected by ^{11}B NMR spectroscopy after 21 h at 20 °C in toluene. The experimental evidence therefore suggested that **3** may be dehydrocoupled by precatalysts **1** and **7** by similar or related mechanisms, both based on an initial intramolecular dehydrogenation process.

The ability of the in situ generated Fe catalyst to dehydrocouple multiple batches of **3** was also explored. Following the conversion of **3** to **4** in 20 min with 5 mol % of precatalyst **7** in toluene, another equivalent of **3** was then added. This was completely dehydrocoupled in a further 10 min. This process was repeated an additional three times before any significant decrease in rate was observed.

6. Mechanistic Insight into the Dehydrocoupling of $Me_2NH{\cdot}BH_3$ (3) Using $Cp_2Fe_2(CO)_3(MeCN)$ (7) as a Precatalyst. As noted previously, the need to photoirradiate precatalysts **1** and **2** to achieve turnover complicated the detailed analysis of the reactions. This was especially true in the case of **2** as continual photoirradiation was required. Precatalyst **7** therefore provided an important opportunity to probe the mechanism of dehydrogenation in more detail as catalysis was achieved without photoirradiation. Furthermore, it is likely that the initial unsaturated species formed from precatalyst **7** is identical to that for **1** and further insight into the detailed mechanism for the latter species would be accessible.

The reaction of precatalyst **7** with amine–borane **3** in toluene was monitored by ^{11}B NMR spectroscopy, using a reduced catalyst loading of 0.5 mol % to achieve a reaction time scale appropriate for accurate monitoring (~110 min). Analysis of the reaction every 2 min over 0.5 h provided clear evidence for a significant induction period prior to the observation of catalytic activity (Figure 7, plot **a**). In addition, the reaction solution was observed to change from light green to light brown in color with significant bubbling, concomitant with the detection of **4** and **5** by ^{11}B NMR spectroscopy. Repeat experiments under the same conditions demonstrated reproducibility in these observations, with an average induction period of 22 min over five runs.

The observation of an induction period and a color change upon the onset of active catalysis strongly suggested, as anticipated, that the initial MeCN adduct is not the active catalyst in the dehydrogenation reaction. It is probable that the initial process in solution would involve MeCN dissociation. Evidence in support of this assertion was given by the aforementioned suppression of catalysis when the dehydrogenation of **3** using **7** is attempted in MeCN, where ligand dissociation is presumably prevented (see section 5).

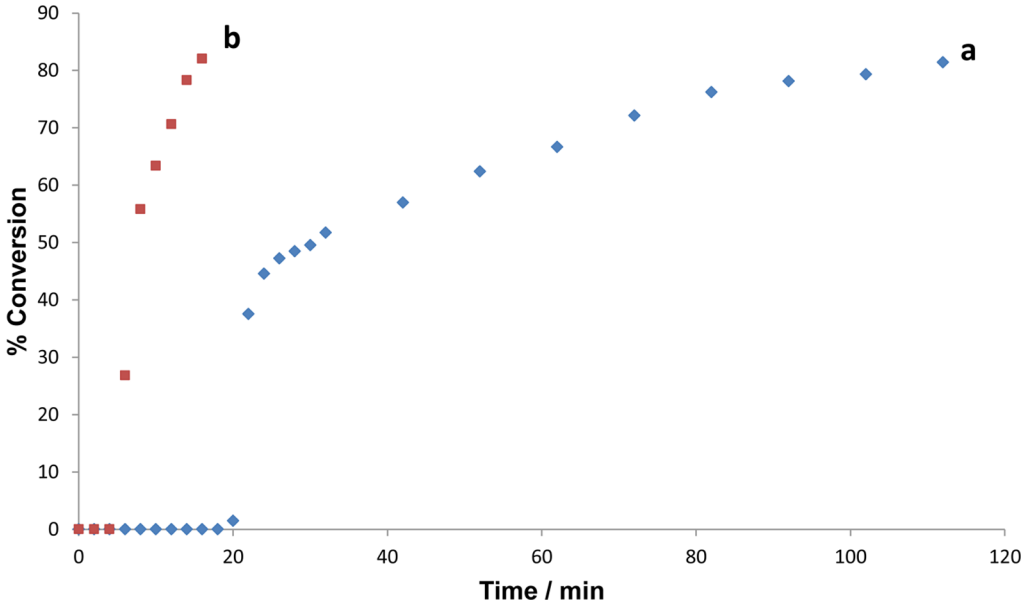

Figure 7. Conversion of $Me_2NH{\cdot}BH_3$ (**3**) to $[Me_2N{-}BH_2]_2$ (**4**) with time for a 0.5 mol % loading of $Cp_2Fe_2(CO)_3(MeCN)$ (**7**) in toluene at 20 °C. Conversions based on analysis of ^{11}B NMR spectra. Plot **a** shows a standard catalytic run in which **3** and **7** are added to solution at the same time. Plot **b** shows the catalytic run in which **7** was stirred with an excess of $Me_3N{\cdot}BH_3$ (**16**) for 30 min before addition of **3**.

dx.doi.org/10.1021/ja410129j | J. Am. Chem. Soc. 2014, 136, 3048–3064

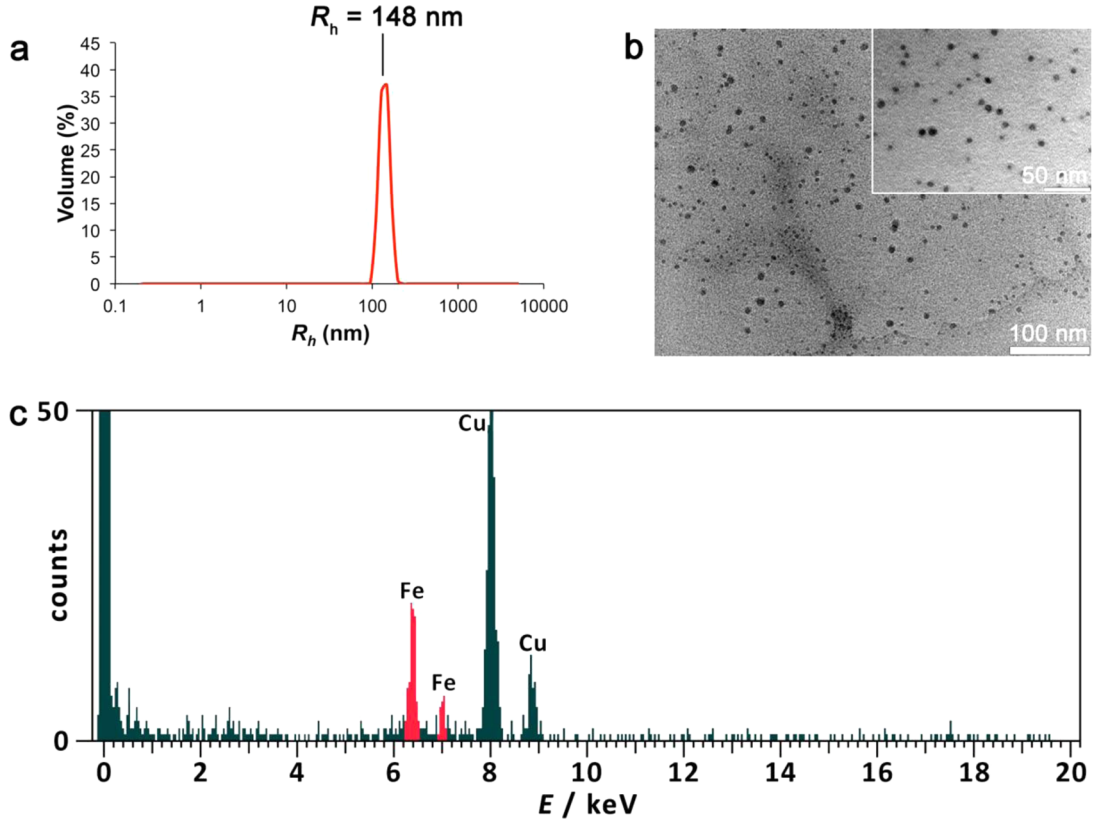

Figure 8. (a) DLS particle size distribution by volume. (b) TEM micrograph showing evidence for the colloidal nature of the reaction of $Me_2NH{\cdot}BH_3$ (**3**) and $Cp_2Fe_2(CO)_3(MeCN)$ (**7**) (5 mol %) (insert: high magnification image). (c) Energy-dispersive X-ray spectroscopic (EDX) analysis of the particles (probe size diameter: 35 nm). The Cu in the EDX spectrum arises from the TEM grid on which the sample was analyzed.

The results suggest that it is highly likely that the active catalyst formed by **7** is heterogeneous in nature and might be formed simply via reduction of the initial metal complex by the amine–borane substrate, a process for which there is substantial literature precedent.[87,112] As noted above, nanoparticles based on various metals have been shown to dehydrocouple amine–boranes under hydrolytic[69,113] and nonhydrolytic conditions,[49] which lends more support to the proposal that Fe nanoparticles are the active catalyst formed via in situ reduction of precatalyst **7**. To further investigate this hypothesis, an attempt was made to reduce **7** to form Fe nanoparticles prior to the addition of **3**. Precatalyst **7** (0.5 mol %) was stirred in toluene with an excess of $Me_3N{\cdot}BH_3$ (**16**), which was used as the reducing agent due to its solubility in toluene and also due to the lack of a feasible dehydrocoupling pathway. After 30 min, which was comparable to the induction period observed in the reaction of amine–borane **3** with precatalyst **7**, amine–borane **3** was added and the reaction was analyzed every 2 min by ^{11}B NMR spectroscopy. In this case, a far shorter induction period (between 0 and 6 min over three runs) and an improved reaction rate were observed (Figure 7, plot **b**). This further supported the hypothesis that Fe nanoparticles formed in situ by the reduction of **7** by **3** were the true active catalyst.

As discussed previously in section 4, various tests to differentiate homo- and heterogeneous catalytic processes have been devised.[92,93] The ability of PMe_3 to selectively poison the catalyst derived from **7** was also investigated. Amine–borane **3** was reacted with **7** (5 mol %) in toluene for 30 min, by which time ^{11}B NMR spectroscopy showed complete conversion to **4** as expected. Next, 0.1 equiv of PMe_3 (with regard to the total iron content in the reaction mixture) was then added before the subsequent addition of a further equivalent of **3**. Analysis by ^{11}B NMR spectroscopy showed no further dehydrogenation over 120 min indicating that a substoichiometric quantity of PMe_3 completely suppressed the activity of the catalyst. Repeating the experiment using CS_2 as the catalyst poison yielded a similar result. Furthermore, as a control experiment, the reaction was repeated with omission of the poisoning agent. In this case, the second equivalent of amine–borane **3** was rapidly dehydrocoupled by the active catalyst generated in situ from **7** affording cyclic diborazane **4** as the final product within 10 min. The reaction was then repeated with addition of a substoichiometric quantity of PMe_3 to **7** before the addition of **3**. Precatalyst **7** (5 mol %) and 0.1 equiv of PMe_3 were added to toluene and stirred for 10 min before addition of amine–borane **3**. Analysis of the reaction mixture after 30 min by ^{11}B NMR spectroscopy indicated no dehydrocoupling had occurred.

The reaction mixture containing **7** (5 mol %) and amine–borane **3** in toluene was also analyzed by DLS as previously described for the reaction with precatalyst **1**. As for the case of **1**, this indicated the existence of a colloidal solution, albeit containing particles of slightly larger size (R_h = 148 nm, Figure 8a). Broadly consistent with this result was the observation by TEM of iron-containing[114] particles ranging in diameter from ca. 10–30 nm with the average size calculated as 10 nm (Figure 8b,c), which are slightly larger values than those found in the reaction with **1**.[115,116]

dx.doi.org/10.1021/ja410129j | J. Am. Chem. Soc. 2014, 136, 3048–3064

DLS and TEM control experiments were also performed for precatalyst **7** in MeCN solution, as previously described for **1** in THF. Although some particulates were observed in the TEM images (Figure S4 (b), Supporting Information), the surface density was much lower than that found in the reaction with **3**, and there was no evidence for a significant concentration of such species by DLS (see Figure S3, Supporting Information). We therefore conclude that, as for **1**, the nanoparticles observed in the reaction with **3** are native, although we cannot completely exclude the possibility that some of those observed by TEM arise due to reduction of the precatalyst by the electron beam.

As with the case of **1**, UV−vis spectroscopy was again used in an attempt to detect iron nanoparticles with **7** as the dehydrocoupling catalyst. Although significantly different spectra were recorded for **7** and for the reaction mixture with **3** consisting of a substantial broadening of absorptions through the visible spectrum to lower wavelengths, this is consistent with, rather than convincing evidence for, the presence of a surface plasmon resonance absorption of metallic nanoparticles (see Figures S6 and S7, Supporting Information; for a UV−vis spectrum of Fe nanoparticles see section 7 and Figure S11, Supporting Information).[97]

After determining that the active catalyst for the dehydrocoupling reactions catalyzed by **1** and **7** was heterogeneous, it was of interest to reinvestigate the Fe carbonyl dimer complex $Fe_2(CO)_9$ (**8**) for which we previously obtained negative results as a precatalyst. The inherent photosensitivity of this complex, which functions as a convenient source of nanoparticulate Fe, made it very surprising that no dehydrocoupling activity was observed under the catalyst screening conditions.[117] Upon reinvestigation, **8** (5 mol %) was photoirradiated together with amine−borane **3** in THF at 20 °C for 24 h. Analysis by ^{11}B NMR spectroscopy again showed minimal dehydrogenation to afford **4** (ca. 1%). The reaction mixture was then analyzed by DLS, which indicated the formation of a colloidal solution with relatively large particles (R_h = 550 nm), and this was further confirmed by TEM (Figure S14, Supporting Information). It is likely that the inactivity of **8** is therefore due to the large size of the particles and consequently low concentration of active surface sites.

7. Investigation of Fe Nanoparticles as an Amine−Borane Dehydrocoupling Catalyst. To support the assertion that Fe nanoparticles are the active catalytic species in dehydrocoupling reactions of **3** mediated by **7** and **1**, it was important to investigate the activity of independently prepared Fe nanoparticles toward the dehydrogenation of **3**. Among the examples of Fe nanoparticles reported in the literature, two distinct classes are apparent, defined by the presence or lack of ancillary ligands to prevent agglomeration. We therefore set out to prepare representative examples of both classes as a means of probing the general reactivity of Fe nanoparticles in this context.

The reactivity of stabilizer-free Fe nanoparticles was initially investigated with a sample prepared via reduction of $FeCl_3$ by $NaBH_4$ in aqueous media using the method of Klabunde and co-workers.[118] Due to the likelihood of metal-catalyzed hydrolysis of amine−boranes in aqueous media, the nanoparticles were isolated by cannula filtration before washing successively in degassed H_2O, EtOH, and dry Et_2O and finally drying under high vacuum for 2 h. The stabilizer-free Fe nanoparticles were isolated as a black solid and characterized by TEM, which showed the formation of large Fe aggregates (1 μm) (Figure S9, Supporting Information). The catalytic activity of the resulting magnetic solids was then investigated through reaction with amine−borane **3** in toluene and THF at a 5 mol % loading. In both cases no evidence of dehydrogenation was apparent over 4 h at 20 °C by ^{11}B NMR spectroscopy.

In the case of ligand-supported Fe nanoparticles, both phosphines and amines are commonly employed in the ancillary role, as well as various polymers.[119,120] We employed the method of Amiens and co-workers, who demonstrated the stabilization of Fe nanoparticles by poly(2,6-dimethyl-1,4-phenylene oxide).[121] It was postulated that this polyaryl ether stabilizer would be suitably non-interacting with the amine−borane substrate so as to not complicate the reaction. The Fe nanoparticles were prepared via the reduction of $Fe(N[SiMe_3]_2)_2$ by H_2 at 110 °C in the presence of the stabilizer. The Fe nanoparticles, which were isolated as a black solid, were characterized by TEM and UV−vis spectroscopy. Fe nanoparticles were observed by TEM (ca. 30 nm, Figure S10, Supporting Information), although these were larger than the nanoparticles generated from **1** or **7**. UV−vis spectroscopy also clearly showed a surface plasmon resonance typically indicative of nanoparticles (Figure S11, Supporting Information). However, once again, no catalytic reactivity was observed on treatment of toluene or THF solutions of **3** with a 5 mol % loading of these nanoparticles at 20 °C after 4 h.

The last examples of ligand-stabilized nanoparticles that were synthesized were those published by Bönnemann et al.[122,123] In this case, the Fe nanoparticles were prepared via the reduction of $FeCl_2$ by $[N(Octyl)_4][BEt_3H]$ at 20 °C in THF. The $[N(octyl)_4]^+$ cation stabilized Fe nanoparticles (**17**), which were isolated as a dark gray solid, were then characterized by TEM, which showed that, unlike the cases of the other methods, small nanoparticles (~3 nm) were formed (Figure S12, Supporting Information). Treatment of **3** with 5 mol % loading of **17** in toluene at 20 °C over 20 h led to 40% conversion of **3** to **4** was detected by ^{11}B NMR spectroscopy. A similar conversion was observed when the reaction was repeated in THF, and although the activity is significantly less than that detected using precatalyst **1** and **7**, this may be a consequence of the different surface ligation. Interestingly, there were also mechanistic similarities between the dehydrocoupling of amine−borane **3** with **17** and for precatalysts **1** and **7**. Analysis of the reaction mixture by ^{11}B NMR spectroscopy showed that the aminoborane **5** was formed, whereas linear diborazane **6** was not detected (Figure S13, Supporting Information). Further insight was given by the very low activity of the **17** toward the dehydrocoupling of **6**, suggesting that a similar mechanism was in operation for all the heterogeneous Fe(0) catalysts investigated.[124]

■ DISCUSSION

The observation of the monomeric aminoborane **5** as an intermediate in the dehydrogenation reactions catalyzed with $[CpFe(CO)_2]_2$ (**1**) and $Cp_2Fe_2(CO)_3(MeCN)$ (**7**), in contrast to those with $CpFe(CO)_2X$ (X^- = I^- (**2**), Cl^- (**12**), OTf^- (**14**)) and also $[CpFe(CO)_2(THF)][X]$ X^- = $[BF_4]^-$ or $[SbF_6]^-$ (**13a** and **13b**) as a precatalyst, suggests a potential similarity in the reaction mechanisms in the case of the former dinuclear species. Mechanistic studies for **1** involving poisoning experiments and TEM and DLS analysis of reaction solutions suggested that this species was reduced on photoirradiation in the presence of **3** to generate Fe nanoparticles as the true

dx.doi.org/10.1021/ja410129j | J. Am. Chem. Soc. 2014, 136, 3048−3064

Scheme 10. Possible Routes to Forming an Unsaturated Fe Complex Using $[CpFe(CO)_2]_2$ (1) and $Cp_2Fe_2(CO)_3(MeCN)$ (7)

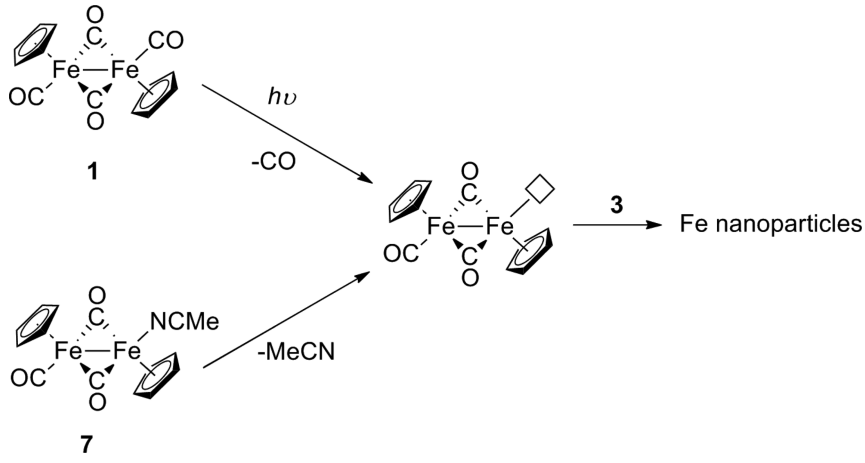

Scheme 11. Possible Mechanism for the Dehydrogenation of $Me_2NH{\cdot}BH_3$ (3) To Afford $Me_2N{=}BH_2$ (5) on a Metal Nanoparticle Surface and Subsequent "Off-Metal" Dimerization To Yield 4

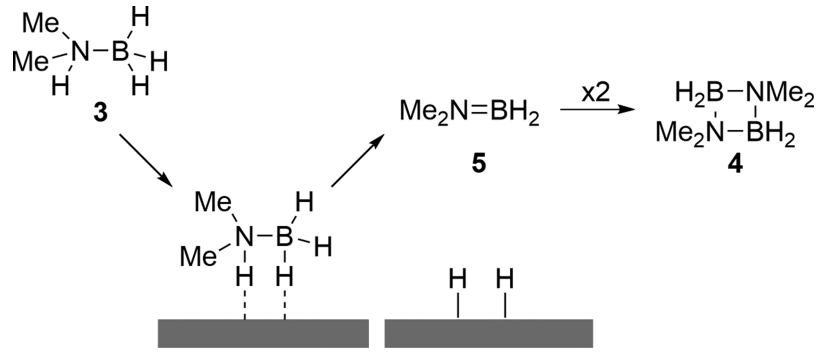

heterogeneous catalyst. The discovery of the precatalyst **7**, which does not require photoirradiation to mediate the dehydrocoupling of **3**, facilitated more detailed mechanistic studies. Significantly, these revealed the presence of an induction period associated with the reduction step, a key signature for a heterogeneous catalytic process. These observations support the assertion that **1** and **7** are each reduced to Fe nanoparticles, the active catalytic species in the dehydrogenation of **3**, probably via the coordinatively unsaturated complex $[Cp_2Fe_2(CO)_3]$ in a process that requires the presence of **3** (Scheme 10). This process requires photoirradiation in the case of **1** to remove CO, unlike the case for **7**. It is possible that the CO generated in the case of **1** can coordinate to the surface of the Fe nanoparticles. This could reduce their catalytic activity and might explain the lower rate found for **1** compared to **7** for the catalytic dehydrocoupling of **3**. The reduction of **1** and **7** to Fe(0) may involve intermediates similar to those noted based on studies of the photochemistry of **1** with H_2 and main group hydride species by Bitterwolf et al.[125] where E-H bond activation followed by subsequent rearrangement afforded iron-containing complexes such as $CpFe(CO)_2H$.

As discussed previously, two different basic metal-mediated mechanisms for the dehydrocoupling of amine−borane **3** have been postulated in the literature (Scheme 2). In the first, 1 equiv of H_2 is removed from a single molecule of **3** in a metal-catalyzed intramolecular process to yield the monomeric aminoborane **5** as a short-lived intermediate. The aminoborane subsequently dimerizes in a spontaneous "off-metal" process to give **4** (although it is also possible that the transformation can also be metal-mediated).[72] This mechanistic pathway has been invoked for various catalyst systems, although in the majority of cases the aminoborane **5** is observed only in small quantities due to the slow generation of the species and relativity short solution lifetime.[39,56−58,72,126,127]

In the second of these mechanisms, the linear diborazane **6** is formed as the key intermediate and is subsequently dehydrogenated in a second "on-metal" process to give the final product. This is exemplified in the recent study from our group and collaborators of the $[Cp_2Ti]$-mediated dehydrogenation of secondary amine−boranes, in which experimental observations and kinetic studies strongly implicate the linear diborazane **6** as the key intermediate.[44] Diborazane **6** has also been postulated as an intermediate in the dehydrogenation of **3** in various other catalyst systems.[42,52,57,71,126,128]

In the case of photoactivated **1**, the observation of significant quantities of the monomeric aminoborane **5** during the dehydrogenation of **3**, coupled with the minimal reactivity of this catalyst toward isolated **6**, makes this one of the most convincing examples of a dehydrocoupling of **3** solely via the monomeric aminoborane. Interestingly, a trend develops when comparing the intermediates detected using precatalysts **1** or **7** to other amine−borane dehydrocoupling catalysts believed to be heterogeneous in nature. In the case of skeletal Ni,[51] the major pathway for the dehydrogenation of **3** was an "off-metal" process affording **4** via aminoborane **5**, in accordance with reactivity observed when using in situ or ex situ generated Fe nanoparticles. Furthermore, the extensively studied [Rh(1,5-

dx.doi.org/10.1021/ja410129j | J. Am. Chem. Soc. 2014, 136, 3048−3064

Scheme 12. Possible Two-Stage Mechanism for the Dehydrocoupling of $Me_2NH{\cdot}BH_3$ (3) with Iron Precatalyst $CpFe(CO)_2I$ (2)

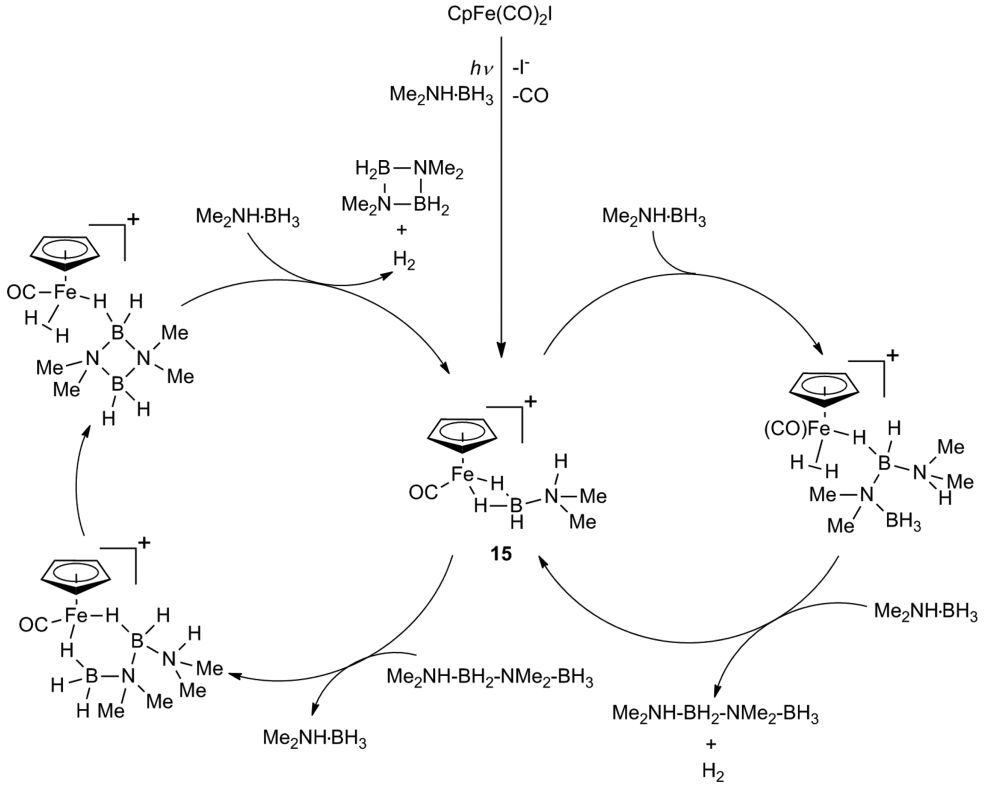

cod)Cl]$_2$ system,[41,42,73,129−134] which has been reported to generate Rh colloids and clusters during the dehydrocoupling of **3**, also proceeds mainly via aminoborane **5**, although small amounts of linear diborazane **6** were also detected (Figure S15, Supporting Information). It is possible that the mechanism involving **5** as an intermediate is favored in cases where the active catalyst is heterogeneous as dehydrogenation of a single molecule of **3** affording aminoborane **5** (Scheme 11) may be more likely to occur on a metal surface than two molecules of amine−borane **3** reacting via an intermolecular dehydrocoupling step to give linear diborazane **6**. Interestingly, the presence of small but significant amounts of **6** in the Ni and [Rh(1,5-cod)Cl]$_2$ systems may suggest that a second, perhaps homogeneous, mechanism may also operate as a minor component.[135]

In contrast to the cases of **1** and **7**, experimental observations indicate the formation of linear diborazane **6** in the dehydrocoupling of aminoborane **3** catalyzed by Fe precatalyst **2** results from a homogeneous mechanism.[136] Photolysis in this instance is continuously required to achieve catalytic turnover and does not result in the formation of detectable Fe nanoparticles by TEM and DLS analysis. In this case, it is highly likely that **2** dehydrocouples **3** via an initial intermolecular coupling event to form **6**, which then subsequently dehydrogenates in an "on-metal" step to afford **4**. This process is strongly reminiscent of the extensively studied [Cp_2Ti]-mediated dehydrocoupling mechanism for **3**[44,54] and a similar, two-stage catalytic cycle may operate (Scheme 12). Experimental studies of the catalytic dehydrocoupling of **3** mediated by **2**, and also **13a** and **13b** and **14**, together DFT calculations provide tentative support for the proposed intermediacy of photogenerated [$CpFe(CO)]^+$ which readily binds **3** to form **15**. In the case of precatalyst **2**, photogenerated I^- can presumably recombine with the active catalyst leading to the need for continuous irradiation to achieve catalytic turnover. This explanation is supported by the observation that continuous irradiation is not necessary in the cases of precatalysts **13a** and **13b**, which possess weakly coordinating anions.

An important yet challenging issue to address is the relationship between the precatalyst structure and the dehydrocoupling mechanism detected. Why are the mechanisms involving precatalysts **1** and **7** heterogeneous whereas that of **2** is homogeneous? We speculate that the low formal oxidation state, Fe(I), and the binuclear structures in **1** and **7**, which already possess Fe−Fe interactions, may contribute to their ease of reduction to Fe nanoparticles in the presence of the reductant **3**. On the other hand, entry into the homogeneous catalytic manifold proposed in this work for **2** is probably enabled by the presence of the electronegative iodine substituent which makes heterolytic cleavage of an iron-ligand bond possible thereby maintaining the Fe(II) oxidation state. Although not analyzed in detail in this work, we assume that Fe(II) complexes **12**, **13a**, **13b**, and **14** catalyze the dehydrocoupling of **3** by analogous mechanisms to that for **2** (Scheme 12) and that these mononuclear Fe(II) species are also resistant to reduction for similar reasons.

Finally, one other result warrants further comment. Why is $Fe_2(CO)_9$, an obvious source of Fe nanoparticles, inactive as a precatalyst? It appears that this complex decomposes to Fe nanoparticles so rapidly that large Fe nanoparticles are formed (Figure S14, Supporting Information) with low reactivity as a result of their relatively low surface area. In contrast, the smaller, catalytically active nanoparticles generated from complexes **1** and **7** possess cyclopentadienyl ligands whose loss may constitute the rate limiting step in this process. This

dx.doi.org/10.1021/ja410129j | J. Am. Chem. Soc. 2014, 136, 3048−3064

explanation is supported by the lack of reactivity observed with most of the Fe nanoparticles independently generated by reductive techniques in the literature (see section 7).[137] Only when the size was very small (ca. 3 nm) and $[N(Octyl)_4]^+$ cations were used as stabilizers (Figure S12, Supporting Information) was significant activity for the dehydrocoupling of **3** apparent. Thus, unstabilized Fe nanoparticles formed large micrometer-scale aggregates (Figure S9, Supporting Information) and showed no catalytic activity. These results and our in situ DLS and TEM studies suggest that the **1** and **7** function as sources of small iron nanoparticles (≤10 nm) that are presumably generated during the reaction induction period, which was detected in the case of **7**. The controlled generation of nanoparticles is likely facilitated by the presence of cyclopentadienyl ligands which are much less labile than CO substituents.[138] Presumably, the nanoparticles formed possess sufficient surface stabilization to prevent rapid aggregation as their catalytic activity is maintained after irradiation is halted (in the case of **1**) and recycling is possible.

SUMMARY AND CONCLUSIONS

Amine−borane dehydrogenation/dehydrocoupling precatalysts based on the earth-abundant metal iron have been developed. Detailed studies have demonstrated that either heterogeneous or homogeneous mechanisms may operate depending on subtle structural variations of the precatalyst. The iron carbonyl complexes **1** and **2** were found to be efficient precatalysts for the dehydrocoupling/dehydrogenation of the amine−borane **3** upon UV photoirradiation at ambient temperature. In situ analysis of the reaction mixtures indicated that different, two-step mechanisms operate in each case. Thus, precatalyst **1** dehydrocoupled **3** via the aminoborane **5** which then cyclodimerized to give the cyclodiborazane **4** via an off-metal process. In contrast, the reaction with precatalyst **2** proceeded via the linear diborazane **6** as the key intermediate, affording **4** as the final product after a second metal-mediated step. The complex **7**, formed by photoirradiation of **1** in MeCN, was found to be a more highly active dehydrocoupling catalyst for **3**, and photoactivation was not required. Detailed mechanistic studies indicated that the active catalysts generated from precatalyst **7** and also **1** were heterogeneous in nature and consisted of small iron nanoparticles (≤10 nm).[139] In contrast, analogous experimental studies for the case of photoactivated Fe precatalyst **2** suggested that the active catalyst formed in this case was homogeneous. Investigations of this and analogous species (such as **12**, **13a**, **13b**, and **14**) together with DFT studies suggested a two-stage catalytic cycle with amine−borane ligated $[CpFe(CO)]^+$ (**15**) as a key intermediate.

Further work will focus on an investigation of the dehydrocoupling reactivity of the Fe precatalysts toward primary amine−borane adducts and other substrates such as **9** that enable polyaminoborane formation. We also aim to perform further mechanistic work and model compound studies in order to provide further detailed support for the homogeneous mechanism proposed in Scheme 12.

ASSOCIATED CONTENT

Supporting Information

Full experimental details and details of additional experiments. This material is available free of charge via the Internet at http://pubs.acs.org.

AUTHOR INFORMATION

Corresponding Author

ian.manners@bris.ac.uk

Notes

The authors declare no competing financial interest.

ACKNOWLEDGMENTS

J.R.V., A.S., A.P.M.R., G.R.W., and I.M. acknowledge the Engineering and Physical Sciences Research Council (EPSRC) for financial support.

REFERENCES

(1) Baudoin, O. *Chem. Soc. Rev.* **2011**, *40*, 4902−4911.
(2) Fihri, A.; Bouhrara, M.; Nekoueishahraki, B.; Basset, J.-M.; Polshettiwar, V. *Chem. Soc. Rev.* **2011**, *40*, 5181−5203.
(3) Trnka, T. M.; Grubbs, R. H. *Acc. Chem. Res.* **2000**, *34*, 18−29.
(4) Schrock, R. R.; Hoveyda, A. H. *Angew. Chem., Int. Ed.* **2003**, *42*, 4592−4633.
(5) Kress, S.; Blechert, S. *Chem. Soc. Rev.* **2012**, *41*, 4389−4408.
(6) Eisch, J. J. *Organometallics* **2012**, *31*, 4917−4932.
(7) (a) Bolm, C.; Legros, J.; Le Paih, J.; Zani, L. *Chem. Rev.* **2004**, *104*, 6217−254. (b) Fürstner, A.; Martin, R. *Chem. Lett.* **2005**, *34*, 624−629. (c) Bauer, E. B. *Curr. Org. Chem.* **2008**, *12*, 1341−1369.
(8) Bedford, R. B.; Betham, M.; Bruce, D. W.; Danopoulous, A. A.; Frost, R. M.; Hird, M. *J. Org. Chem.* **2006**, *71*, 1104−1110.
(9) Hudson, R.; Hamasaka, G.; Osako, T.; Yamada, Y. M. A.; Li, C.-J.; Uozami, Y.; Moores, A. *Green. Chem.* **2013**, *15*, 2141−2148.
(10) (a) Bullock, R. M. *Science* **2013**, *342*, 1054−1055. (b) Jagadeesh, R. V.; Surkus, A.-E.; Junge, H.; Pohl, M.-M.; Radnik, J.; Rabeah, J.; Huan, H.; Schünemann, V.; Brückner, A.; Beller, M. *Science* **2013**, *342*, 1073−1076. (c) Friedfield, M. R.; Shevlin, M.; Hoyt, J. M.; Krska, S. W.; Tudge, M. T.; Chirik, P. J. *Science* **2013**, *342*, 1076−1080. (d) Zuo, W.; Lough, A. J.; Li, Y. F.; Morris, R. H. *Science* **2013**, *342*, 1080−1083.
(11) Clark, T. J.; Lee, K.; Manners, I. *Chem.—Eur. J.* **2006**, *12*, 8634−8648.
(12) Less, R. J.; Melen, R. L.; Wright, D. S. *RSC Adv.* **2012**, *2*, 2191−2199.
(13) Waterman, R. *Chem. Soc. Rev.* **2013**, *42*, 5629−5641.
(14) Leitao, E. M.; Jurca, T.; Manners, I. *Nature Chem.* **2013**, *5*, 817−829.
(15) Hutchins, R. O.; Learn, K.; Nazer, B.; Pytlewski, D.; Pelter, A. *Org. Prep. Proced. Int.* **1984**, *16*, 335−372.
(16) Lane, C. F. *Aldrichimica Acta* **1973**, *6*, 51−58.
(17) Bartoli, G.; Bartolacci, M.; Giuliani, A.; Marcantoni, E.; Massaccesi, M. *Eur. J. Org. Chem.* **2005**, 2867−2879.
(18) Pasumansky, L.; Goralski, C. T.; Singaram, B. *Org. Process. Res. Dev.* **2006**, *10*, 959−970.
(19) Kanth, J. V. B. *Aldrichimica Acta* **2002**, *35*, 57−66.
(20) Beachley, O. T., Jr.; Washburn, B. *Inorg. Chem* **1975**, *14*, 120−123.
(21) Staubitz, A.; Robertson, A. P. M.; Manners, I. *Chem. Rev.* **2010**, *110*, 4079−4124.
(22) Stephens, F. H.; Pons, V.; Baker, R. T. *Dalton Trans.* **2007**, 2613−2626.
(23) Smythe, N. C.; Gordon, J. C. *Eur. J. Inorg. Chem.* **2010**, 509−521.
(24) Sutton, A. D.; Burrell, A. K.; Dixon, D. A.; Garner, E. B., III; Gordon, J. C.; Nakagawa, T.; Ott, K. C.; Robinson, P.; Vasiliu, M. *Science* **2011**, *331*, 1426−1429.
(25) Wright, N. R. H.; Berkeley, E. R.; Alden, L. R.; Baker, R. T.; Sneddon, L. G. *Chem Commun.* **2011**, *47*, 3177−3179.
(26) Jaska, C. A.; Manners, I. *J. Am. Chem. Soc.* **2004**, *126*, 2698−2699.
(27) Sloan, M. E.; Staubitz, A.; Lee, K.; Manners, I. *Eur. J. Org. Chem.* **2011**, *2011*, 672−675.

(28) Yang, X.; Fox, T.; Berke, H. *Chem. Commun.* **2011**, *47*, 2053−2055.
(29) Yang, X.; Fox, T.; Berke, H. *Org. Biomol. Chem.* **2012**, *10*, 852−860.
(30) Robertson, A. P. M.; Leitao, E. M.; Manners, I. *J. Am. Chem. Soc.* **2011**, *133*, 19322−19325.
(31) Leitao, E. M.; Stubbs, N. E.; Robertson, A. P. M.; Helten, H.; Cox, R. J.; Lloyd-Jones, G. C.; Manners, I. *J. Am. Chem. Soc.* **2012**, *134*, 16805−16816.
(32) Yang, X.; Zhao, L.; Fox, T.; Wang, Z.-X.; Berke, H. *Angew. Chem., Int. Ed.* **2010**, *49*, 2058−2062.
(33) Staubitz, A.; Soto, A. P.; Manners, I. *Angew. Chem., Int. Ed.* **2008**, *47*, 6212−6215.
(34) Dietrich, B. L.; Goldberg, K. I.; Heinekey, D. M.; Autrey, T.; Linehan, J. C. *Inorg. Chem.* **2008**, *47*, 8583−8585.
(35) Staubitz, A.; Sloan, M. E.; Robertson, A. P. M.; Friedrich, A.; Schneider, S.; Gates, P. J.; Schmedt auf der Günne, J.; Manners, I. *J. Am. Chem. Soc.* **2010**, *132*, 13332−13345.
(36) Liu, Z.; Song, L.; Zhao, S.; Huang, J.; Ma, L.; Zhang, J.; Lou, J.; Ajayan, P. M. *Nano Lett.* **2011**, *11*, 2032−2037.
(37) Ewing, W. C.; Marchione, A.; Himmelberger, D. W.; Carroll, P. J.; Sneddon, L. G. *J. Am. Chem. Soc.* **2011**, *133*, 17093−17099.
(38) There are also many examples in which main group metals have been used to dehydrocouple amine−borane adducts. See: (a) Liptrot, D. L.; Hill, M. S.; Mahon, M. F.; MacDougall, D. J. *Chem.—Eur. J.* **2010**, *16*, 8508−8515. (b) Hill, M. S.; Kocick-Koln, G.; Robinson, T. P. *Chem. Commun.* **2010**, *46*, 7587−7589. (c) Spielmann, J.; Piesik, D. F.-J.; Harder, S. *Chem.—Eur. J.* **2010**, *16*, 8307−8318. (d) Spielmann, J.; Harder, S. *Dalton Trans.* **2011**, *40*, 8314−8319. (e) Appelt, C.; Slootweg, J. C.; Lammertsma, K.; Uhl, W. *Angew. Chem., Int. Ed.* **2013**, *52*, 4256−4259. (f) Hansmann, M. M.; Melen, R. L.; Wright, D. S. *Chem. Sci.* **2011**, *2*, 1554−1559. (g) Crowley, H. J.; Holt, M. S.; Melen, R. L.; Rawson, J. M.; Wright, D. S. *Chem. Commun.* **2011**, *47*, 2682−2684. (h) Less, R. J.; Simmonds, H. R.; Dane, S. B. J.; Wright, D. S. *Dalton Trans.* **2013**, *42*, 6337−6343.
(39) Kawano, Y.; Uruichi, M.; Shimoi, M.; Taki, S.; Kawaguchi, T.; Kakizawa, T.; Ogino, H. *J. Am. Chem. Soc.* **2009**, *131*, 14946−14957.
(40) Kakizawa, T.; Kawano, Y.; Naganeyama, K.; Shimoi, M. *Chem. Lett.* **2011**, *40*, 171−173.
(41) Jaska, C. A.; Temple, K.; Lough, A. J.; Manners, I. *Chem. Commun.* **2001**, 962−963.
(42) Jaska, C. A.; Temple, K.; Lough, A. J.; Manners, I. *J. Am. Chem. Soc.* **2003**, *125*, 9424−9434.
(43) Clark, T. J.; Russell, C. A.; Manners, I. *J. Am. Chem. Soc.* **2006**, *128*, 9582−9583.
(44) Sloan, M. E.; Staubitz, A.; Clark, T. J.; Russell, C. A.; Lloyd-Jones, G. C.; Manners, I. *J. Am. Chem. Soc.* **2010**, *132*, 3831−3841.
(45) Dallanegra, R.; Robertson, A. P. M.; Chaplin, A. B.; Manners, I.; Weller, A. S. *Chem. Commun.* **2011**, *47*, 3763−3765.
(46) Denney, M. C.; Pons, V.; Hebden, T. J.; Heinekey, D. M.; Goldberg, K. I. *J. Am. Chem. Soc.* **2006**, *128*, 12048−12049.
(47) Keaton, R. J.; Blacquiere, J. M.; Baker, R. T. *J. Am. Chem. Soc.* **2007**, *129*, 1844−1845.
(48) Baker, R. T.; Gordon, J. C.; Hamilton, C. W.; Henson, N. J.; Lin, P.-H.; Maguire, S.; Murugesu, M.; Scott, B. L.; Smythe, N. C. *J. Am. Chem. Soc.* **2012**, *134*, 5598−5609.
(49) Sonnenberg, J. F.; Morris, R. H. *ACS Catalysis* **2013**, 1092−1102.
(50) Jiang, Y.; Blacque, O.; Fox, T.; Frech, C. M.; Berke, H. *Organometallics* **2009**, *28*, 5493−5504.
(51) Robertson, A. P. M.; Suter, R.; Chabanne, L.; Whittell, G. R.; Manners, I. *Inorg. Chem.* **2011**, *50*, 12680−12691.
(52) Friedrich, A.; Drees, M.; Schneider, S. *Chem.—Eur. J.* **2009**, *15*, 10339−10342.
(53) Vance, J. R.; Robertson, A. P. M.; Lee, K.; Manners, I. *Chem.—Eur. J.* **2011**, *17*, 4099−4103.
(54) Helten, H.; Dutta, B.; Vance, J. R.; Sloan, M. E.; Haddow, M. F.; Sproules, S.; Collison, D.; Whittell, G. R.; Lloyd-Jones, G. C.; Manners, I. *Angew. Chem., Int. Ed.* **2013**, *52*, 437−440.
(55) Luo, Y.; Ohno, K. *Organometallics* **2007**, *26*, 3597−3600.
(56) Pun, D.; Lobkovsky, E.; Chirik, P. J. *Chem. Commun.* **2007**, 3297−3299.
(57) (a) Vogt, M.; de Bruin, B.; Berke, H.; Trincado, M.; Grützmacher, H. *Chem. Sci.* **2011**, *2*, 723−727. (b) Garcia-Vivó, D.; Huergo, E.; Ruiz, M. A.; Travieso-Puente, R. *Eur. J. Inorg. Chem.* **2013**, 4998−5008.
(58) Chapman, A. M.; Haddow, M. F.; Wass, D. F. *J. Am. Chem. Soc.* **2011**, *133*, 8826−8829.
(59) Tang, C. Y.; Thompson, A. L.; Aldridge, S. *J. Am. Chem. Soc.* **2010**, *132*, 10578−10591.
(60) Duman, S.; Ozkar, S. *Int. J. Hydrogen Energ.* **2013**, *38*, 10000−10011.
(61) Zahmakiran, M.; Ozkar, S. *Top. Catal.* **2013**, *56*, 1171−1183.
(62) Kim, S.-K.; Han, W.-S.; Kim, T.-J.; Kim, T.-Y.; Nam, S. W.; Mitoraj, M.; Piekoś, L.; Michalak, A.; Hwang, S.-J.; Kang, S. O. *J. Am. Chem. Soc.* **2010**, *132*, 9954−9955.
(63) Chaplin, A. B.; Weller, A. S. *Angew. Chem., Int. Ed.* **2010**, *49*, 581−584.
(64) Butera, V.; Russo, N.; Sicilia, E. *Chem.—Eur. J.* **2011**, *17*, 14586−14592.
(65) Paul, A.; Musgrave, C. B. *Angew. Chem., Int. Ed.* **2007**, *46*, 8153−8156.
(66) García-Vivó, D.; Huergo, E.; Ruiz, M. A.; Travieso-Puente, R. *Eur. J. Inorg. Chem.* **2013**, *28*, 4998−5008.
(67) Dallanegra, R.; Chaplin, A. B.; Weller, A. S. *Angew. Chem., Int. Ed.* **2009**, *48*, 6875−6878.
(68) Marziale, A. N.; Friedrich, A.; Klopsch, I.; Drees, M.; Celinski, V.; Schmedt auf der Günne, J.; Schneider, S. *J. Am. Chem. Soc.* **2013**, *135*, 13342−13355.
(69) Dinç, M.; Metin, Ö.; Özkar, S. *Catal. Today* **2012**, *183*, 10−16.
(70) Examples of iron-catalyzed dehydrogenation/dehydrocoupling of other B−N containing substrates have been reported. For an example of Fe-catalyzed dehydrogenation of boron−nitrogen heterocycles, see: (a) Luo, W.; Campbell, P. G.; Zakharov, L. N.; Liu, S.-Y. *J. Am. Chem. Soc.* **2011**, *133*, 19326−19329. Also, Fe nanoparticles have been used for the hydrolytic dehydrogenation of **9** to yield borates. See: (b) Aranishi, K.; Jiang, H.-L.; Akita, T.; Haruta, m.; Xu, Q. *Nano Res.* **2011**, *4*, 1233−1241. (c) Qiu, F.; Li, L.; Wang, Y.; An, C.; Xu, C.; Xu, Y.; Wang, Y.; Jiao, L.; Yuan, H. *Int. J. Hydrogen Energy* **2013**, *38*, 7291−7297. (d) Wang, H.-L.; Yan, J.-M.; Wang, Z.-L.; Jiang, Q. *Int. J. Hydrogen Energy* **2012**, *37*, 10229−10235. (e) Qiu, F.; Li, L.; Liu, G.; Wang, Y.; Wang, Y.; An, C.; Xu, Y.; Xu, C.; Wang, Y.; Jiao, L.; Yuan, H. *Int. J. Hydrogen Energy* **2013**, *38*, 3241−3249.
(71) Sewell, L. J.; Lloyd-Jones, G. C.; Weller, A. S. *J. Am. Chem. Soc.* **2012**, *134*, 3598−3610.
(72) Stevens, C. J.; Dallanegra, R.; Chaplin, A. B.; Weller, A. S.; MacGregor, S. A.; Ward, B.; McKay, D.; Alcaraz, G.; Sabo-Etienne, S. *Chem.—Eur. J.* **2011**, *17*, 3011−3020.
(73) Chen, Y.; Fulton, J. L.; Linehan, J. C.; Autrey, T. *J. Am. Chem. Soc.* **2005**, *127*, 3254−3255.
(74) For other relevant studies, see: (a) Johnson, H. C; Robertson, A. P. M.; Chaplin, A. B.; Sewell, L. J.; Thompson, A. L.; Haddow, M. F.; Manners, I.; Weller, A. S. *J. Am. Chem. Soc.* **2011**, *133*, 11076−11078. For a study with the related phosphine-borane adducts see (b) Huertos, M. A.; Weller, A. S. *Chem. Sci.* **2013**, *4*, 1881−1888.
(75) It is noteworthy that pentamethylation of the Cp rings (as in **1***) led to a reduction in catalytic activity. Furthermore, it was also of interest that $Fe_2(CO)_9$ (**8**) was found to be almost completely inactive. See the Discussion section.
(76) $HB(NMe_2)_2$ is observed during dehydrocoupling reactions, and similar compounds ($HB(NR_2)_2$) have been characterized in other research. For a recent paper detailing some examples, see: Helten, H.; Robertson, A. P. M.; Staubitz, A.; Vance, J. R.; Haddow, M. F.; Manners, I. *Chem.—Eur. J.* **2012**, *18*, 4665−4680.
(77) Recently, Morris et al. reported that $FeBr_2$ was found to dehydrocouple $H_3N{\cdot}BH_3$ (**9**) in the presence of KO^tBu: see ref 49. Sonnenberg, J. F.; Morris, R. H. *ACS Catalysis* **2013**, 1092−1102.

(78) Nöth, H.; Thomas, S. *Eur. J. Inorg. Chem.* **1999**, *1999*, 1373–1379.
(79) *Comprehensive Organometallic Chemistry*, 2nd ed.; Shriver, D. F. B., Michael, I., Ed.; Pergamon Press: New York, 1995; Vol. 7.
(80) Caspar, J. V.; Meyer, T. J. *J. Am. Chem. Soc.* **1980**, *102*, 7794–7795.
(81) Meyer, T. J.; Caspar, J. V. *Chem. Rev.* **1985**, *85*, 187–218.
(82) Dixon, A. J.; George, M. W.; Hughes, C.; Poliakoff, M.; Turner, J. J. *J. Am. Chem. Soc.* **1992**, *114*, 1719–1729.
(83) Douglas, T. M.; Chaplin, A. B.; Weller, A. S. *J. Am. Chem. Soc.* **2008**, *130*, 14432–14433.
(84) Douglas, T. M.; Chaplin, A. B.; Weller, A. S.; Yang, X.; Hall, M. B. *J. Am. Chem. Soc.* **2009**, *131*, 15440–15456.
(85) Alcaraz, G.; Vendier, L.; Colt, E.; Sabo-Etienne, S. *Angew. Chem., Int. Ed.* **2010**, *49*, 918–920.
(86) Alcaraz, G.; Sabo-Etienne, S. *Angew. Chem., Int. Ed.* **2010**, *49*, 7170–7179.
(87) (a) Staubitz, A.; Robertson, A. P. M.; Sloan, M. E.; Manners, I. *Chem. Rev.* **2010**, *110*, 4023–4078. (b) Stephens, F. H.; Baker, R. T.; Matus, M. H.; Grant, D. J.; Dixon, D. A. *Angew. Chem. Int. Ed.* **2007**, *46*, 746–749.
(88) Hai-Shan, D.; Roberts, B. P. *Tetrahedron Lett.* **1992**, *33*, 6169–6172.
(89) Dang, H.-S.; Roberts, B. P. *J. Chem. Soc., Perkin Trans.* **1993**, 891–898.
(90) Bitterwolf, T. E. *Coord. Chem. Rev.* **2000**, *206–207*, 419–450.
(91) Photoirradiation of precatalyst **1** in THF, followed by addition of amine–borane **3** led to no observable reaction over 4 h by ^{11}B NMR spectroscopy.
(92) Widegren, J. A.; Finke, R. G. *J. Mol. Cat. A: Chem.* **2003**, *198*, 317–341.
(93) Widegren, J. A.; Bennett, M. A.; Finke, R. G. *J. Am. Chem. Soc.* **2003**, *125*, 10301–10310.
(94) Crabtree, R. H. *Chem. Rev.* **2012**, *112*, 1536–1554.
(95) Based on recent work by Amiens and co-workers, the Fe nanoparticles are also anticipated to contain significant amounts of boron (which is difficult to detect by EDX analysis). These workers showed that treatment of Fe(II) salts with amine–boranes led to Fe nanoparticles containing 15–25% B based on EXAFS and Mössbauer spectroscopy. Mechanisms of formation involving the reactions with aminoborane intermediates or products at the nanoparticle nucleation stage or with the Fe nanoparticles themselves were proposed. See: Pellelier, F.; Ciuculescu, D.; Mattei, J.-G.; Lecante, P.; Casanove, M.-J.; Schmitz-Antoniak, C.; Amiens, C. *Chem.—Eur. J.* **2013**, *19*, 6021–6026.
(96) DLS affords a translational diffusion coefficient for the particle(s), which is then translated in to an effective hydrodynamic size by means of the Stokes–Einstein equation. This relationship assumes that the particles are non-interacting hard spheres diffusing through viscous liquid.
(97) Njagi, E. C.; Huang, H.; Stafford, L.; Genuino, H.; Galindo, H. M.; Collins, J. B.; Hoag, G. E.; Suib, S. L. *Langmuir* **2011**, *27*, 264–271.
(98) It should be noted that the wavelength of the peak associated to the surface plasmon resonance is directly related to the size of the nanoparticles and the metal they contain.
(99) Alway, D. G.; Barnett, K. W. *Inorg. Chem.* **1978**, *17*, 2826–2831.
(100) Allen, D. M.; Cox, A.; Kemp, T. J.; Sultana, Q. *Inorg. Chim. Acta* **1977**, *21*, 191–194.
(101) It should be noted that a third conceivable photoactivated process would involve homolytic cleavage of the Fe–I bond to form a $CpFe(CO)_2$ radical and I$^{\bullet}$. This route is improbable, however, as various studies have demonstrated this process to be unfavored. Furthermore, the formation of $CpFe(CO)_2$ radical would presumably lead to the formation of **1**, and under photoirradiation this would lead to dehydrogenation of **3** via aminoborane **5**, which is not observed in this case. For further information on $CpFe(CO)_2$ radicals, see refs 99 and 100.
(102) Pan, X.; Philbin, C. E.; Castellani, M. P.; Tyler, D. R. *Inorg. Chem.* **1988**, *27*, 671–676.
(103) In an attempt to detect $[CpFe(CO)(PMe_3)_2]^+$ by ^{31}P NMR spectroscopy, PMe_3 was added to $CpFe(CO)_2I$ (**2**) under photolysis. However, further investigation indicated that PMe_3 also reacted with **2** under ambient conditions to give $[CpFe(CO)(PMe_3)_2]^+$ and $[CpFe(PMe_3)_3]^+$. See the Supporting Information.
(104) An atmosphere of CO will most likely suppress any loss of CO from the Fe precatalyst, although the observed lack of conversion may also be due to catalyst poisoning.
(105) $CpFe(CO)_2Cl$ (**12**) was used instead of $CpFe(CO)_2I$ (**2**) because iodide is not covered by the basis set used (6-311G(d,p)). Both complexes showed similar reactivity in toluene meaning that this exchange was appropriate.
(106) See the Supporting Information for further details.
(107) $[CpFe(CO)_2]_2$ (**1**) has previously be shown to be active dehydrocoupling catalyst towards a range of amine–borane adducts in a preliminary publication. See ref 53.
(108) Zhang, S.; Brown, T. L. *Organometallics* **1992**, *11*, 4166–4173.
(109) Labinger, J. A.; Madhavan, S. *J. Organomet. Chem.* **1977**, *134*, 381–389.
(110) Hamilton, C. W.; Baker, R. T.; Staubitz, A.; Manners, I. *Chem. Soc. Rev.* **2009**, *38*, 279–293.
(111) In a separate experiment, amine–borane **3** was stirred in neat MeCN for 20 h at 20 °C and no reactivity was observed when the reaction mixture was analyzed by ^{11}B NMR spectroscopy.
(112) Babu Kalidindi, S.; Sanyal, U.; Jagirdar, B. R. *ChemSusChem* **2011**, *4*, 317–324.
(113) (a) Yan, J.-M.; Zhang, X.-B.; Han, S.; Shioyama, H.; Xu, Q. *Angew. Chem., Int. Ed.* **2008**, *47*, 2287–2289. (b) Clark, T. J.; Whittell, G. R.; Manners, I. *Inorg. Chem.* **2007**, *46*, 7522–7527.
(114) See ref 95.
(115) The distribution of particle sizes derived from DLS and TEM may differ for a number of reasons. First, DLS is reliant on the scattered light intensity from an ensemble of particles, which is dominated by that arising from the larger species. TEM, however, has no such bias and individual particles can be observed, but a large number of measurements are needed for a meaningful average to be obtained. Thus, particles of the size observed by TEM (10–30 nm) may have been present in the DLS sample, albeit in a concentration that was too small to be detected in the presence of larger species (148 nm). Conversely, as only a selection of the particles present in colloidal solution collects on the substrate during TEM sample preparation, larger particles may have drifted off the grid or serendipitously gathered in regions that were not examined. Such problems in identifying all the species present in a colloidal solution by TEM will often be encountered when complex mixtures are present, and this situation is exaggerated here due to the presence of additional reactant and/or product. The evaporation of solvent may lead to the crystallization of these compounds, which may then obscure objects of interest, and also other drying effects, such as particle aggregation, which prevent the images from truly representing the particles in solution. Furthermore, the reducing nature of the electron beam and the unavoidable exposure of the substrate to air on introduction to the microscope serve to divorce the particles from their native environment and may result in structural changes on performing the TEM experiment. DLS, on the other hand, can be performed under the standard reaction conditions (excluding photoirradiation) and, therefore, represents a truer picture of the overall particle size distribution. When the appropriate TEM control experiments are performed, however, there is no doubt that *both* methods suggest that the reaction mixture is heterogeneous in nature. Also see ref 96 and the Supporting Information.
(116) As suggested by a reviewer, filtration of the reaction mixture prior to analysis by DLS could lead to aggregation. This could explain the differences in sizes obtained by DLS and TEM. Further preliminary experiments were performed to investigate the effect of filtration on the size of Fe(0) nanoparticles observed. In the case of the unfiltered samples, uninterpretable data was obtained. This is likely

due to dust particles and other contaminants making it impossible to detect the very small nanoparticles. TEM was also obtained, and comparison between the unfiltered and filtered cases suggested that some aggregation did take place in the latter case.
(117) Indeed, the absence of significant activity with $Fe_2(CO)_9$ (**8**), a ready source of colloidal Fe, led us to suggest in our preliminary communication that the catalytic dehydrocoupling of **3** by **1** under UV irradiation was a homogeneous process. See ref 53, footnote 20.
(118) Glavee, G. N.; Klabunde, K. J.; Sorensen, C. M.; Hadjipanayis, G. C. *Inorg. Chem.* **1995**, *34*, 28−35.
(119) Alexandridas, P. *Chem. Eng. Technol.* **2011**, *34*, 15−28.
(120) Virkutyte, J.; Varma, R. S. *Chem. Sci.* **2011**, *2*, 837−846.
(121) Margeat, O.; Dumestre, F.; Amiens, C.; Chaudret, B.; Lecante, P.; Respaud, M. *Prog. Solid State Chem.* **2005**, *33*, 71−79.
(122) Boennemann, H.; Brinkmann, R.; Neiteler, P. *Appl. Organometal. Chem* **1994**, *8*, 361−378.
(123) Boennemann, H.; Braun, G.; Brijoux, W.; Brinkmann, R.; Schulze Tilling, A.; Seevogel, K.; Siepen, K. *J. Organomet. Chem.* **1996**, *520*, 143−162.
(124) It is again worth noting that treatment of **3** with anhydrous $FeCl_2$ (the precursor to **17**) in either toluene or THF resulted in no dehydrocoupling after 4 h when analysed by ^{11}B NMR spectroscopy. See Table 1.
(125) Bitterwolf, T. E.; Linehan, J. C.; Shade, J. E. *Organometallics* **2000**, *19*, 4915−4917.
(126) Robertson, A. P. M.; Suter, R.; Chabanne, L.; Whittell, G. R.; Manners, I. *Inorg. Chem.* **2011**, *50*, 12680−12691.
(127) Hill, M. S.; Kociok-Köhn, G.; Robinson, T. P. *Chem. Commun.* **2010**, *46*, 7587−7589.
(128) Beweries, T.; Hansen, S.; Kessler, M.; Klahn, M.; Rosenthal, U. *Dalton Trans.* **2011**, *40*, 7689−7692.
(129) Jaska, C. A.; Manners, I. *J. Am. Chem. Soc.* **2004**, *126*, 9776−9785.
(130) Jaska, C. A.; Manners, I. *J. Am. Chem. Soc.* **2004**, *126*, 1334−1335.
(131) Fulton, J. L.; Linehan, J. C.; Autrey, T.; Balasubramanian, M.; Chen, Y.; Szymczak, N. K. *J. Am. Chem. Soc.* **2007**, *129*, 11936−11949.
(132) Zahmakiran, M.; Özkâr, S. *Inorg. Chem.* **2009**, *48*, 8955−8964.
(133) Metin, Ö.; Mazumder, V.; Özkâr, S.; Sun, S. *J. Am. Chem. Soc.* **2010**, *132*, 1468−1469.
(134) Metin, Ö.; Suman, S.; Dinç, M.; Özkâr, S. *J. Phys. Chem. C* **2011**, *115*, 10736−10743.
(135) Although the heterogeneous catalysts appear to operate through mechanisms that form **5** rather than **6** based on the current literature, homogeneous catalysts seem to be more flexible and can participate in mechanisms that involve either species as an intermediate.
(136) It should be further noted that various catalysts have been shown to dehydrocouple amine−borane **3** by both metal-mediated mechanisms. For example, reaction of **3** with Schneider's homogeneous Ru catalyst led to dehydrogenation to afford **4**. Both aminoborane **5** and linear diborazane **6** were detected by ^{11}B NMR spectroscopy, although **6** was seemingly the favored intermediate. See ref 52.
(137) We have also shown that skeletal Fe is inactive as a precatalyst for the dehydrogenation of **3**; see ref 51.
(138) Bayram, E.; Linehan, J. C.; Fulton, J. L.; Roberts, J. A. S.; Szymczak, N. K.; Smurthwaite, T. D.; Özkar, S.; Balasubramanian, M.; Finke, R. G. *J. Am. Chem. Soc.* **2011**, *133*, 18889−18902.
(139) See ref 95.